https://doi.org/10.5194/amt-2022-331
Preprint. Discussion started: 20 December 2022

Atmospheric Measurement Techniques Discussions

Long-term validation of Aeolus L2B wind products at Punta Arenas, Chile and Leipzig, Germany.

Holger Baars[1], Joshua Walchester[1,3], Elizaveta Basharova[1,3], Henriette Gebauer[1,3], Martin Radenz[1], Johannes Bühl[1], Boris Barja[2], Ulla Wandinger[1], and Patric Seifert[1]

[1]Leibniz Institute for Tropospheric Research (TROPOS), Leipzig, Germany
[2]Atmospheric Research Laboratory, University of Magallanes, Punta Arenas, Chile
[3]University of Leipzig, Leipzig, Germany

Correspondence: Holger Baars, baars@tropos.de

Abstract. Ground-based observations of horizontal winds have been performed in Leipzig (51.12 N, 12.43 E), Germany, and at Punta Arenas (53.35 S, 70.88 W), Chile, in the framework of the German initiative EVAA (Experimental Validation and Assimilation of Aeolus observations) with respect to the validation of the Mie and Rayleigh wind products of Aeolus (L2B data). In Leipzig, at the Leibniz Institute for Tropospheric Research (TROPOS), radiosondes have been launched on each Friday for the Aeolus overpasses (ascending orbit) since mid of May 2019. In Punta Arenas, scanning Doppler cloud radar observations have been performed in the frame of the DACAPO-PESO campaign (dacapo.tropos.de) for more than 3 years from end 2018 until end 2021. We present two case studies and long-term statistics of the horizontal winds derived with the ground-based reference instruments compared to Aeolus Horizontal Line-of-Sight (HLOS) winds. It was found that the deviation of the Aeolus HLOS winds from the ground-reference is usually of Gaussian shape which allowed the use of the median bias and the scaled median absolute deviation (MAD) for the determination of the systematic and random error of Aeolus wind products, respectively. The case study from August 2020 with impressive atmospheric conditions in Punta Arenas shows that Aeolus is able to also capture strong wind speeds up to more than 100 m/s. The long-term validation has been performed for all product baselines since the change to the second laser (called FM-B) in June 2019 until summer 2022 and also partly for the era of the first laser (FM-A).

The long-term validation showed that the systematic error of the Aeolus wind products could be significantly lowered with the changes introduced into the processing chain (different baselines) during the mission lifetime. While in the early mission phase, systematic errors of more than 2 m/s (absolute values) were observed for both wind types (Mie cloudy and Rayleigh clear), these biases could be reduced with the algorithm improvements, such as the introduction of the correction for temperature fluctuations at the main telescope of Aeolus (M1 temperature correction) with Baseline 09. Hence, since Baseline 10, a significant improvement of the Aeolus data was found leading to a low bias (close to 0 m/s) and nearly similar values for the mid-latitudinal sites on both hemispheres. The random errors for the wind products were first decreasing with increasing baseline but later increasing again due to the performance losses of the Aeolus emitter. However, the systematic error is only slightly affected by this issue, so that one can conclude that the uncertainty introduced by the reduced atmospheric return signal received by Aeolus is mostly affecting the random error.

https://doi.org/10.5194/amt-2022-331
Preprint. Discussion started: 20 December 2022

Atmospheric Measurement Techniques Discussions

Even when considering these issues, we can confirm the general validity of Aeolus observations during its lifetime. This proves the general concept of this space explorer mission to perform active wind observations from space.

1 Introduction

In 2018, the Aeolus satellite of the European Space Agency (ESA) was launched with the goal to improve weather forecast through global measurements of wind profiles (Stoffelen et al., 2005; Reitebuch, 2012). To obtain vertical resolved wind measurements around the globe, the High-Spectral-Resolution (HSR) Doppler lidar ALADIN (Atmospheric Laser Doppler Instrument) was installed on board. It has been the first time, that a lidar with Doppler capabilities as well as with high spectral resolution capabilities has been operated in space. Given this unique and novel space-borne technique, it is possible to actively measure vertical profiles of the line-of-sight (LOS) wind in clear sky by using air molecules as tracer (Rayleigh methodology) and in cloudy atmospheric regions, using cloud particles as tracer (Mie methodology - de Kloe et al., 2016; Tan et al., 2008; Baars et al., 2020b). The profiles of line-of-sight wind velocity (35°off nadir) are then projected to a plane parallel to the Earth's surface to obtain the horizontal line-of-sight (HLOS) wind, i.e., one wind component of the horizontal wind vector (near west-east direction). Besides that, the technology can be used to obtain profiles of aerosol and cloud optical properties as spin off product (e.g., Baars et al., 2021; Flament et al., 2021; Siomos et al., 2021).

The main goal of the mission is the assimilation of the wind products into numerical weather prediction (NWP) models to demonstrate its benefit for weather forecast (Stoffelen et al., 2006; ESA, 2008, 2018). This has meanwhile be done at several meteorological centers (Rennie et al., 2021; Rani et al., 2022; Martin et al., 2022) and a clear positive impact on forecast skills has been reported (ECMWF, 2019a, b)

Given the novelty, extensive validation efforts have been needed to verify the observations, detect unforeseen challenges (instrument and processing wise) and develop respective correction or calibration updates in order to make such a data assimilation within near-real time (less than 3 hours) possible at all. For this reason, an intense feedback from Cal/Val teams was desired and obtained to work together with the Aeolus DISC (Data, Innovation, and Science Cluster) and ESA itself on the improvement and stability of instrument and products.

Since the launch in 2018, several challenges were identified by DISC and ESA according to the feedback from the Cal/Val teams (e.g., Krisch et al., 2020). Some important issues are listed in the following:

- Initially lower laser energy with a more rapid decline than expected (Simonelli et al., 2019; Reitebuch et al., 2020; Lux et al., 2020b),
- Switch to second laser with different beam characteristics which were also changing over time (Straume et al., 2020),
- Occurrence of increased background noise for some pixels (hot pixels) on the ACCD (Accumulation Charge-Coupled Devices) of ALADIN (Weiler et al., 2021a),
- Changes in the wind accuracy according to differences in temperature at the main telescope mirror of ALADIN (Weiler et al., 2021b).

https://doi.org/10.5194/amt-2022-331
Preprint. Discussion started: 20 December 2022


Atmospheric Measurement Techniques Discussions

DISC and ESA have worked hard on these features to improve the stability of the instrument and its products. This has been a prerequisite for the direct assimilation. As the above-mentioned issues influence the use, e.g., the assimilation, of the Aeolus data, continuous and long-lasting validation becomes very important. Most of the operational validation of Aeolus products was performed with NWP models (using of course also assimilated measurements - Chen et al., 2021; Hagelin et al., 2021; Martin et al., 2021; Liu et al., 2022; Zuo et al., 2022) while a direct validation with dedicated measurements have been rare or rather covering only a short period and usually only a certain geographic region (Baars et al., 2020a; Witschas et al., 2020; Lux et al., 2020a; Baars et al., 2020b; Chen et al., 2021; Martin et al., 2021; Belova et al., 2021; Iwai et al., 2021; Zuo et al., 2022; Wu et al., 2022; Geiß et al., 2022; Lux et al., 2022b; Witschas et al., 2022) .

The Leibniz Institute for Tropospheric Research (TROPOS) performed direct, long-term Aeolus-dedicated measurements of the wind vector at two distinct locations in the framework of the cooperation project EVAA (Baars et al., 2020a, Experimental Validation and Assimilation of Aeolus observations) between the Ludwig-Maximilians-University Munich, the German Aerospace Center (DLR), the German Weather Service (DWD) and TROPOS. In Leipzig, Germany (51°N, 12°E), dedicated radiosondes were launched for the weekly overpass on Aeolus' ascending orbit since 2019, while in Punta Arenas, Chile (53.1°S, 70.9°W), continuous remote-sensing observations of LACROS (Radenz et al., 2021) served as one of the very rare Southern Hemispheric Aeolus validation measurements (Ratynski et al., 2022; Zuo et al., 2022). Namely, scanning Doppler cloud radar data, which have been collected in the framework of the DACAPO-PESO campaign (Radenz et al., 2021) since November 2018, were used for validation activities besides occasional radiosonde launches at the local airport.

In the work presented here, we want to assess the performance of Aeolus and its wind products for the entire period of its nominal lifetime, i.e. 3 years, by using our long-term reference measurements. We also intend to evaluate the potential improvements of the wind products by the introduction of new algorithm versions (baselines) into the operational retrieval chain. We thus aim for analysing the overall performance of Aeolus and the improvements introduced by new processor versions and calibration strategies based on two single sites located in the Northern and Southern Hemispheric mid-latitudes.

The paper is structured as follows: In Section 2, the experimental setup including the campaign locations and instrumentation is described. In Section 3, we explain the methodology applied to derive horizontal wind from the ground-based remote sensing instrument and our validation strategy with respect to Aeolus. Selected case studies are discussed in Sec. 4 to explain the methodology and show already some potentials and limitations of Aeolus. Finally, long-term statistics taking also the different algorithm versions of Aeolus into account, are presented and discussed concerning the Aeolus performance in Sec. 5. Last but not least, the drawn conclusions are presented.

https://doi.org/10.5194/amt-2022-331
Preprint. Discussion started: 20 December 2022

Atmospheric Measurement Techniques Discussions

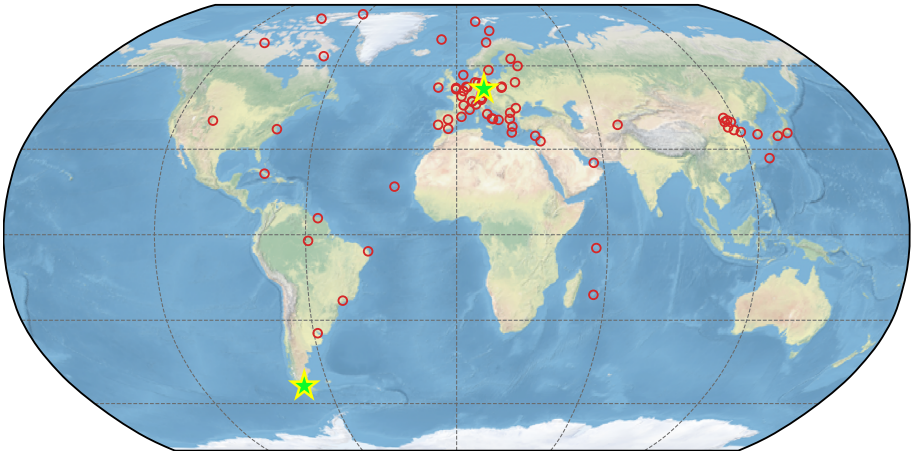

Figure 1. Map of Aeolus Cal/Val stations. The ones considered in this work highlighted as green-yellow stars.

2 Experimental setup

2.1 Campaign locations

2.1.1 Punta Arenas, Chile

The remote-sensing supersite LACROS (Leipzig Aerosol and Cloud Remote Observations System) has been operated at Punta Arenas, Chile (53.14°S, 70.88°W) from November 2018 to November 2021 for the DACAPO-PESO campaign (Radenz et al., 2021). Thereby, one of the first multi-year ground-based remote sensing data set in the Southern mid-latitudes was obtained. The LACROS instrumentation comprises a PollyXT Raman-polarization-lidar (Engelmann et al., 2016; Baars et al., 2016), a CHM15kx ceilometer, a MIRA-35 scanning cloud Doppler radar (Görsdorf et al., 2015), a HATPRO microwave radiometer, and a Streamline Doppler lidar. Additionally, radiosondes could be launched at the airport of Punta Arenas for dedicated objectives.

Punta Arenas is an ideal location for the validation of Aeolus in terms of wind conditions: A strong circumpolar flow is a characteristic feature of the Southern Ocean with the southern tip of South America being the only barrier in the latitude band from 47°S to 63°S. Low pressure systems embedded in this flow usually pass through the Drake passage south of Punta Arenas causing prevailing wind directions between south-west and north-west. A comprehensive description of the meteorological conditions is provided in Radenz et al. (2021).

Aeolus overpasses considered for the validation were on Wednesday, ca. 23:26 UTC on the ascending orbit, and on Thursdays, at around 09:56 UTC on the descending orbit. For the presented study, the scanning Doppler cloud radar has been primarily used and is thus explained in more detail in Section 2.2.

https://doi.org/10.5194/amt-2022-331
Preprint. Discussion started: 20 December 2022


Atmospheric Measurement Techniques Discussions

2.1.2 Leipzig, Germany

At the ACTRIS (Aerosol, Clouds and Trace Gases Research Infrastructure) site of Leipzig, Germany (51.35° N, 12.43°E), Aeolus Cal/Val activities were focused on dedicated radiosonde launches (see Sec. 2.2.2). These launches took place for the ascending orbit of Aeolus on Friday evening at around 16:50 UTC.

Leipzig is located in central Europe being in the intermediate state between maritime and continental climate. Prevailing winds are usually westerlies, but due to wave activities winds from all direction can be observed. Leipzig is located in the low-land area. No orographical obstacles are around the city, making it a perfect location for the validation of Aeolus.

2.2 Instrumentation

2.2.1 Scanning Doppler cloud radar

Continous measurements were conducted with a 35 GHz Doppler cloud radar of type Metek MIRA35 (Görsdorf et al., 2015). Once per hour, the stare mode (vertical profiling) was interrupted for a Range-Height-Indicator (RHI) and Plan Position Indicator (PPI, also called VAD - Variable Azimuth Display) scan. Only the PPI scans are considered for the horizontal wind retrieval. A pulse repetition frequency of 5000 Hz gives a maximum unambiguous radial velocity of 10.56 m/s, while the range resolution of 31.17 m is determined by the pulse length of 208 ns. Frequent cloud occurrence over Punta Arenas makes this instrument a perfect tool for retrievals of horizontal wind profiles, particularly during austral winter (Seifert et al., 2020; Radenz et al., 2021). The methodology for retrieving wind information from scanning Doppler remote sensing instruments is described in more detail in Sec. 3.1.

2.2.2 Radiosonde

Radiosondes of type Vaisala RS41 (Jauhiainen et al., 2014; Jensen et al., 2016) were launched at Leipzig each Friday for the regular Aeolus evening overpass (on its ascending orbit) since May 2019. The RS41 delivers profiles of temperature, humidity, pressure, wind speed and direction. The uncertainty for the wind products is estimated to be between 0.4 and 1 m/s for the wind velocity and 1° for the wind direction based on calculations of the Global Climate Observing System Reference Upper-Air Network (GRUAN, Dirksen et al., 2014). Even though these estimations are based on Vaisala radiosonde type RS92, there is no significant difference in the uncertainty between both radiosonde types as they are based on the same technique to derive wind velocity and direction (Jensen et al., 2016). A bigger gap in coverage occurred during winter 2020/2021 with only sporadic radiosondes (the reason was local access restriction due to COVID-19) but in total more than 125 launches could be completed. These radiosonde profiles were not assimilated so that they can serve as an independent reference for Aeolus products.

For Aeolus overpasses in Punta Arenas, dedicated radiosondes were launched irregularly. The radiosonde type deployed in Punta Arenas was Lockheed Martin LMS6 and delivered next to temperature, humidity and pressure profiles also profiles of wind speed and direction. In total, 41 radiosondes were launched during the 3 years campaign.

https://doi.org/10.5194/amt-2022-331
Preprint. Discussion started: 20 December 2022

Atmospheric Measurement Techniques Discussions

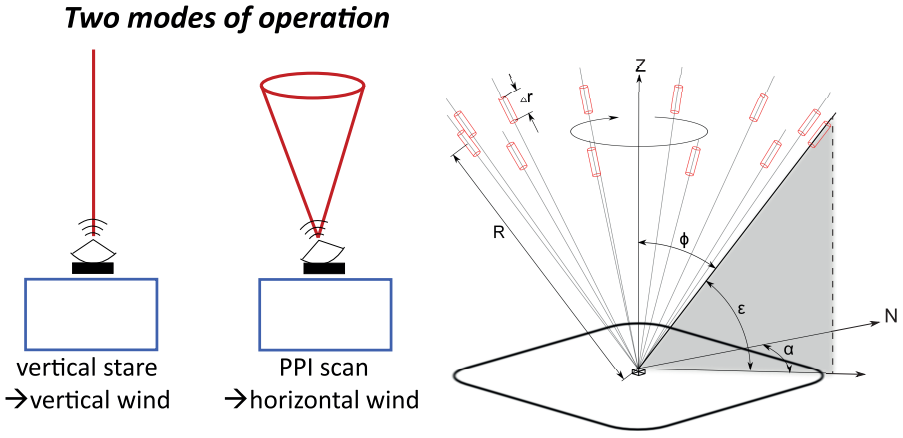

Figure 2. Left: Sketch of the different operating modes of the Doppler cloud radar. Stare mode is used for retrieval of vertical wind speed, while PPI/VAD scans are used to retrieve profiles of horizontal wind speed and direction. Right: Scanning geometry and nomenclature for the PPI/VAD scans as used in this work. The sketch was presented in Päschke et al. (2015) under Creative Commons Attribution 3.0 License and is shown here with permission of the authors.

3 Methodology

3.1 Retrieving horizontal wind profiles from radar

While the remote sensing instruments of TROPOS are usually operating at stare mode (vertical profiling), regular PPI scans have been performed with the Doppler cloud radar to obtain the horizontal wind vector. For these scans, measurements are taken by rotating in azimuth α through a full circle with a fixed elevation angle ϵ (which is set to $85\,°$). A sketch showing the scan patterns is provided in Fig. 2, left. The measured line-of-sight (LOS) Doppler velocity v_{LOS} at the range R and azimuth α is retrieved as the mean of the measured Doppler velocities for a given range band Δr. The Root Mean Square (RMS) of this distribution is used to calculate the uncertainty of v_{LOS}. In the following, we use the notation which is given in Päschke et al. (2015) and which is shown in Fig. 2, right, and neglect that all variables are a function of the range R to allow better reading. The final result is of course depending on R and thus gives a vertical profile. In line with the standard approach of deriving horizontal wind from PPI scans (Browning and Wexler, 1968), the mean horizontal wind speed $v_{\mathrm{advection}}$ can be approximated by fitting the measured v_{LOS} with a trigonometric function of the azimuthal coordinate of the scan corrected for positioning errors ($\alpha_{\mathrm{corrected}}$):

$$v_{\mathrm{projection}}(\alpha_{\mathrm{corrected}}) = v_{\mathrm{advection}} \cdot \cos(\alpha_{\mathrm{corrected}} - \alpha_{\mathrm{wind}}) + B + \sigma. \tag{1}$$

This gives the horizontal wind direction α_{wind} and the horizontal wind speed $v_{\mathrm{advection}}$, with $v_{\mathrm{projection}}$ being the horizontal component projected from v_{LOS}:

$$v_{\mathrm{projection}} = \frac{v_{\mathrm{LOS}}}{\cos(\epsilon)}. \tag{2}$$

https://doi.org/10.5194/amt-2022-331
Preprint. Discussion started: 20 December 2022


Atmospheric Measurement Techniques Discussions

The term σ in Eq. 1 reflects the remaining variation and is aimed to be minimized. For the fit procedure, $v_{\text{advection}}$, α_{wind}, and B are dependent variables, chosen to minimise σ - reflecting the remaining residual. The extra term B reflects the contribution of two factors to the measured Doppler velocity: The divergence in the wind field and the vertical component of the average wind velocity. Both effects are neglected within the following analysis as it is also done for the Aeolus HLOS retrieval.

Three different fit methodologies are used to derive the horizontal wind vector:

1. A least square regression is used to fit $v_{\text{projection}}$ and $\alpha_{\text{corrected}}$ considering also their uncertainties. The fit procedure results in a covariance matrix which is used to calculate the uncertainty. This method is subject to a flaw of Doppler folding by the nature of the measurement process (Ray and Ziegler, 1977). This means, v_{LOS} that exceeds the Nyquist velocity will appear as smaller measured velocity in the opposite direction. Usually, this effect will result in a poor fit quality with a high residual, as the measured $v_{\text{LOS}}(\alpha_{\text{corrected}})$ and thus $v_{\text{projection}}(\alpha_{\text{corrected}})$ will not approximate a trigonometric function, and can thus be discarded.

The other two fit methods that are used to retrieve wind velocities from the raw Doppler velocity data are based on the method by Tabary et al. (2001), which uses the approximation of an azimuthal derivative of the velocity distribution. This method is performed in two different ways.

2. The usual way, as recommended in Tabary et al. (2001), is to approximate the gradient by overlapping piece-wise linear fits centred around each point of the initial distribution. This approach allows to estimate $\partial v_{\text{LOS}}/\partial\alpha_{\text{corrected}}$ which is used to estimate the horizontal wind velocity and direction. This procedure is the second method and is usually consistent with the first method but may lead to higher standard deviations due to removal of data points and the extra stages of calculation. Conversely, when Doppler folding occurs, this method is able to fit to a transformed version of the data with much higher accuracy.

3. The third method is applied because processing large numbers of linear fits as for the second method can sometimes be numerical unstable. This backup method is using the direct differences between consecutive values divided by the azimuthal distance. This approach is consistent with the former ones but leads to correspondingly higher errors because it excludes the averaging that occurs with the linear fit procedure. But on the other hand, if the previous method fails to converge, this (third) Doppler-folding-safe methodology can be used to derive the horizontal wind vector.

All three methods are performed for each range R. In the final data set, a best estimate is then computed which selects the method with the lowest error. This best estimate it then used for the comparison with the Aeolus winds.

3.2 Aeolus validation strategy

For the validation of Aeolus L2B wind products, we use all Aeolus-derived Horizontal Line-of-Sight (HLOS) wind speeds (i.e., at different altitudes) which were assigned to coordinates which are within a radius of 100 km[1] around the measurement site. Accordingly, two overpasses per week fulfilling these conditions were suitable for validation:

[1] 120 km in Punta Arenas after orbit shift in June 2021.

https://doi.org/10.5194/amt-2022-331
Preprint. Discussion started: 20 December 2022

Atmospheric Measurement Techniques Discussions

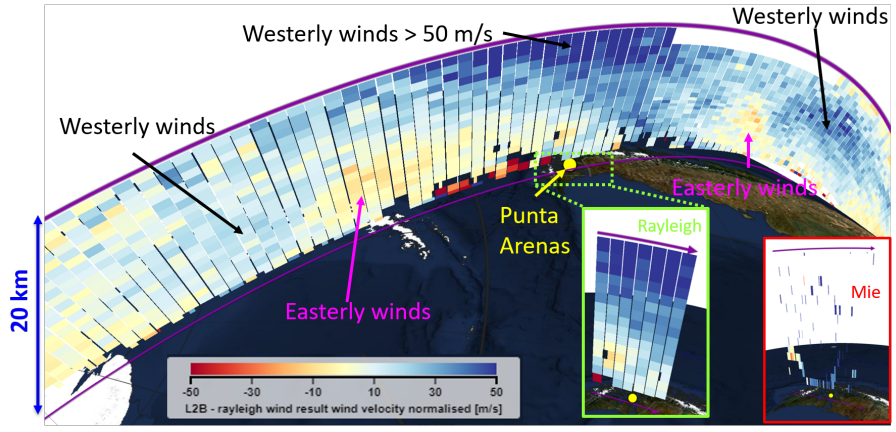

Figure 3. Example for L2B wind curtain around Punta Arenas, Chile, on 30 September 2020 visualized with VIRES (Santillan et al., 2019). The Rayleigh clear wind product is shown for the whole curtain. The Mie wind product (red box) and the Rayleigh wind product (green box) around Punta Arenas is shown in the lower right.

- Punta Arenas: Wednesdays around 23:26 UTC and Thursday around 09:56 UTC,
- Leipzig: Fridays around 16:50 UTC and Sundays around 05:29 UTC.

The validation is done for the so-called Aeolus L2B "Rayleigh clear" wind and "Mie cloudy" wind products. A detailed description of these wind types is given in, e.g., de Kloe et al. (2016) and Baars et al. (2020b). Rayleigh clear winds are delivered at 87 km horizontal resolution while the Mie wind resolution has been mainly at 15 km (setting is flexible).

For a better understanding, an example of the Aeolus Rayleigh wind profiles over Punta Arenas is shown in Fig. 3. On 30 September 2020, strong westerly winds (blueish colors) occurred over Punta Arenas at altitudes above 5 km. Closer to the South Pole, easterly winds (reddish colors) were prevailing. A patchy wind speed pattern was observed close to Punta Arenas near ground, caused by cloud contamination of the Rayleigh winds. Given the example in Fig. 3, one sees that depending on the actual track of Aeolus, 1–3 wind profiles fulfil this criterion of being within 100 km radius of the observational site (see green box in Fig. 3). Considering 15 km vertical resolution for the Mie product since 5 March 2019 (before the resolution was 87 km), one can have up to 13–20 "Mie winds" for one altitude range around the 100 km of the ground-based location (see red box in Fig. 3). For the validation of Aeolus products, the temporal closest observation of the ground-based measurements has been used with allowing a maximum-difference threshold of 1 hour.

Furthermore, we converted the wind speed v_{gb} and direction φ_{gb} obtained with the ground-based (gb, i.e. cloud radar) instruments (see Sec. 3.1) to Aeolus-like HLOS winds $v_{\mathrm{gb_{HLOS}}}$ with the equation described in Baars et al. (2020b):

$$v_{\mathrm{gb_{HLOS}}} = v_{\mathrm{gb}} \cdot \cos(\varphi_{\mathrm{Aeolus}} - \varphi_{\mathrm{gb}}). \tag{3}$$

$\varphi_{\mathrm{Aeolus}}$ is the azimuth angle of Aeolus, which is obtained from the Level 2B data and differs depending on global position. The uncertainties of the ground-based observations were propagated forward. The derived ground-based profiles of HLOS

https://doi.org/10.5194/amt-2022-331
Preprint. Discussion started: 20 December 2022

Atmospheric Measurement Techniques Discussions

Table 1. Overview of the different algorithm version called baseline for the processing of the Aeolus data together with some important additional information.

Baseline	Period	Start date for operational processing	Additional info
B02	Sep 2018 – May 2019	8 Sep 2018	Mie wind res. from 87 km to 15 km in March 2019
B03	May 2019 – June 2019	16 May 2019	
B04	June 2019	14 June 2019	Hot Pixel correction (Weiler et al., 2021a)
B05	June 2019 – September 2019	28 June 2019	Switch to Laser FM-B
B06	June 2019 – October 2019	5 September 2019	
B07	October 2019 – April 2020	31 Oct 2019	
B08	April 2020	2 April 2020	
B09	April 2020 – July 2020	20 April 2020	M1 temp. correction (Weiler et al., 2021b), public data release
B10*	June 2019 – Oct 2020	2019 reprocessed since 9 July 2020 operational	
B11*	June 2019 – May 2021	8 October 2020	
B12	May 2021 – Dec 2021	26 May 2021	Orbit shift in June 2021
B13	Dec 2021 – Mar 2022	6 December 2021	
B14	Mar 2022 – Sep 2022	29 March 2022	

*reprocessed FM-B data set (Baseline 11) - it covers the period June 28, 2019 to October 10, 2020, *Baseline 10: Aeolus FM-B data set in Baseline 10 which covers the early FM-B data from end of June to December 2019

wind were then averaged to the Aeolus range bins thickness to allow a one-to-one comparison. By doing so, we do not discuss here the small-scale wind variability within the relatively large Aeolus range bins but rather concentrate on performance of the space-borne instrument.

During the lifetime of Aeolus, several algorithm versions of the processing chain (so-called baselines) were released and applied. Some of them in operational mode, some of them to reprocess parts of historical Aeolus data. Thus, for certain dates in the Aeolus data set, several versions exist (processed with different baselines) while for other periods only one baseline was applied. An overview of the different baselines of Aeolus covering the observational period of our ground-based reference measurements (i.e., up to summer 2022) is given in Table 1. Two major steps for boosting the performance of Aeolus were made. With Baseline 04, the so-called hot pixel correction (Weiler et al., 2021a) was introduced. Before that, single pixels on the ACCD of Aeolus had a higher dark current and thus biased the retrieved winds. A second important step was the introduction of the correction with respect to changes in the telescope temperature of Aeolus (Weiler et al., 2021b). This was done with Baseline 09 and also should have brought a significant improvement of the performance of the Aeolus winds.

The switch from laser FM-A to Laser FM-B was performed on 12 June 2019 until 28 June 2019 and led to Baseline 05.

https://doi.org/10.5194/amt-2022-331
Preprint. Discussion started: 20 December 2022


Atmospheric Measurement Techniques Discussions

However, a new response calibration needed to be applied which was obtained in August 2019 and led to Baseline 06. The FM-B data since 28 June 2019 was reprocessed under the same baseline. In June 2021, the orbit of Aeolus was shifted to favor the ground-based observations in Cabo Verde during the Joint Aeolus Tropical Atlantic Campaign (JATAC, Fehr et al., 2021). After that date, distances of the measured Aeolus wind to the ground-based reference stations have been different and as a result we increased the maximum radius for Punta Arenas to 120 km to still be able to obtain 2 overpasses per week.

Accounting for changes in units for the uncertainties within the Aeolus products between different baselines, all values for Aeolus horizontal wind speed and errors were transformed into m/s. Other than this unit correction, all baselines were treated equally. Furthermore, beside the provided validity flag within the Aeolus wind products, additional quality measures, i.e. error thresholds for Mie and Rayleigh winds (i.e., 5m/s and 8 m/s, respectively), has been applied. This means that wind products flagged valid but had an error higher than these thresholds were discarded. This is consistent with ESA/ECMWF recommendations (e.g., Rennie and Isaksen, 2020) and studies by other Cal Val teams (e.g., Chen et al., 2021; Geiß et al., 2022).

For the statistical analysis presented in Sec. 5 and 6, the Rayleigh and Mie wind products were treated separately. To obtain statistical metrics, a straight line fit between the ground-reference winds and the Aeolus winds using a orthogonal distance regression (ODR) to include the effects of errors have been computed. We also created histograms of the deviations (reference wind minus Aeolus wind) in the range of -20 to +20 m/s (with higher velocities being assigned to the outside bins) to check for a Gaussian distribution shape.

4 Case studies

4.1 Punta Arenas - 6 February 2020

A schematic overview on how winds are retrieved from the ground-based observations and then compared to Aeolus wind products is shown in Fig. 4 for the case of 6 February 2020, representative for the Southern Hemispheric summer.

The atmospheric conditions above Punta Arenas on this day are presented in Fig. 4, top, left, by means of the Cloudnet Target Categorization (Illingworth et al., 2007; Tukiainen et al., 2020) derived from the vertical starring active remote sensing instrumentation (Cloud radar and Ceilometer) and the passive microwave radiometer. During this day, a nearly cloud-free aerosol layer from ground up to 1.5 km altitude was observed with enough particles to be identified by Cloudnet Target Categorization (dark yellow). Partly, the cloud radar observed a return signal within this aerosol layer which is attributed to insects (red colors). Between 2 and 8 km, clear sky conditions (white color) were found while ice clouds (dark grey) occurred sporadically above 8 km altitude.

Vertical profiles of the horizontal wind vector from the Doppler cloud radar were therefore available when clouds were existing - see Fig. 4, center. The Aeolus overpass on this day was at 09:48 UTC. Thus, the closest wind profile of the Doppler Cloud radar (at 09:35 UTC) plus the HLOS profiles extracted from GDAS1[2] data for 9 UTC and 12 UTC were used to compare with

[2]Global Data Assimilation System (GDAS), ARL Archive: GDAS1 data set, available at: https://www.ready.noaa.gov/gdas1.php

https://doi.org/10.5194/amt-2022-331
Preprint. Discussion started: 20 December 2022

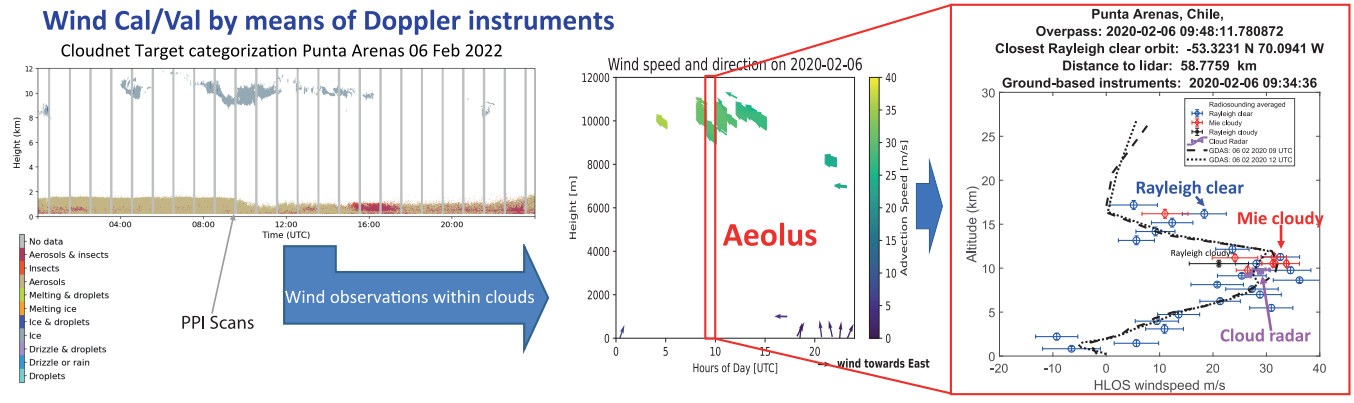

Figure 4. Schematic overview on the methodology used in this paper for the example of 6 February 2020 in Punta Arenas: How are winds retrieved from the Doppler cloud radar and finally compared to Aeolus. Left: Cloudnet Target categorization obtained from the combination of vertical measuring (in stare mode) cloud radar, Ceilometer and microwave radiometer. Center: Resulting winds retrieved with the Doppler cloud radar scans in regions cloud occurrence. Right: Comparison of the HLOS winds from Doppler cloud radar to Aeolus products (Mie cloudy and Rayleigh clear, Baseline 11) for the closest overpass. GDAS model winds are shown as well for comparison.

the Aeolus products (Mie cloudy and Rayleigh clear) as can be seen in Fig. 4, right.

In this example comparison, the advantages and drawbacks of the used reference instrument becomes clear. The cloud radar is only able to retrieve winds in regions were clouds are existent (on this day between 8 and 12 km) and no information can be obtained in clear sky regions. In regions of clouds, however, the winds can be obtained with high frequency and high quality. The GDAS data is of course available in all heights independent of the cloud and aerosol state but in coarser resolution and as a result of assimilation. It is thus no direct validation measure and shown only for consistency checks.

According to Fig. 4, right, an excellent agreement between the ground-based observations and the model data (GDAS) was observed on this day. Aeolus derived wind profiles within a radius of 100 km have been available in clear air (Rayleigh clear winds) and at top of clouds (Mie cloudy winds). The Mie winds available at 10 to 12 km indicate, thus, the presence of clouds at these altitudes. If the cloud deck would be persistent and optically thick over the 87 km horizontal track, no Aeolus winds would be available below due to the strong light attenuation within the cloud. As this is not the case, a broken cloud deck can be assumed in the 87 km averaged Aeolus observation.

On this specific day in (austral) summer 2020, a good agreement between the Mie cloudy winds and the cloud-radar-derived winds were obtained at an altitude of around 10 km. Also, the delivered Rayleigh clear winds in this altitude region agree well with the radar and also with GDAS. The coexistence of Rayleigh clear and Mie cloudy winds in one altitude range is due to the fact of the broken cloud deck and the defined horizontal radius of 100 km for which all Aeolus products are considered. Above, at 17 km height, however, GDAS and Aeolus disagree strongly for the only one Mie cloudy observation there. The reason for that is yet unclear. Rayleigh clear wind agree within the uncertainty range. Below the cloud deck at around 10 km, Rayleigh clear winds are partly matching the model data (GDAS) but with a tendency of higher Aeolus wind speeds down

https://doi.org/10.5194/amt-2022-331
Preprint. Discussion started: 20 December 2022


Atmospheric Measurement Techniques Discussions

to around 5 km altitude. Deviations within the lowest 3 km might be caused by horizontal inhomogeneity within the 100 km radius around the ground-based station. For the statistics presented below in Sec. 5ff., we use the Doppler cloud radar derived winds and compare them to the equivalent Aeolus HLOS winds. For the example case presented here, this means that a comparison to Mie cloudy winds is possible for the height range around about 11 km as this is the only region for which cloud-radar derived winds and Aeolus Mie cloudy winds do coexist. Rayleigh clear wind comparisons can be done at the same height range (reference measurements from the cloud radar). The regions between the ground and 9 km altitude and above 11 km cannot be covered for the comparison due to the missing ground-based measurement data. We did not aim at a comparison with model data, as this is done regularly at ECMWF (Rennie and Isaksen, 2020; Rennie et al., 2021) and by other validation activities (e.g., Martin et al., 2021; Liu et al., 2022; Chen et al., 2021; Hagelin et al., 2021; Rani et al., 2022). Instead, we concentrate on the direct measurements made at ground and space.

4.2 Punta Arenas - 18 August 2021

The second case study from Punta Arenas presents an observation from the Southern Hemispheric winter. At this day, beside the Doppler radar, also a local radiosonde launch was available.

Atmospheric conditions on this day were remarkable. While considerable normal HLOS wind speeds between 5 and 20 m/s were observed in the troposphere, a steady increase in wind speed was observed above the tropopause leading to a maximum measured wind speed by the radiosonde of more than 360 km/h. This Aeolus-observed wind profile was also present in the GDAS data and thus gives confidence of its reality. The reason for such high wind speeds was a shift of the polar vortex toward South America. As a consequence, a high wind speed band was directly located above Punta Arenas. Its horizontal extent is quite broadly distributed around Punta Arenas as can been seen in Fig. 5. There, the Aeolus Rayleigh clear HLOS wind speed curtain is presented as separate plot in the bottom, right, demonstrating the extent of the high-speed wind band.

The comparison of Aeolus derived HLOS winds with the radiosonde is shown in Fig. 5 and reveals that the Rayleigh clear product above 10 km fits perfectly to the observed radiosonde winds and GDAS products. A considerable deviation was observed only at the top most Aeolus range bin (around 24 km). There, the wind speed measured by Aeolus was considerably lower compared to the radiosonde wind. The reason is not clear but might be simply due to the strong drift of the radiosonde due to the high wind speed. Below the tropopause, the agreement of the Aeolus Mie cloudy winds and Rayleigh clear winds with the radiosonde was excellent as well. The GDAS data, however, shows a significant variation at 8 km between the two profiles at 21 UTC and 00 UTC. This implies that fast changes in HLOS, i.e., in wind speed and direction, have taken place in this atmospheric region. Usually, two full Aeolus Rayleigh wind observations (of 87 km horizontal length in case of Rayleigh clear) per Aeolus height bin lay in the validation radius of 100 km around the ground station and are thus considered for the validation. Having a look at the HLOS observations at around 4.7 km, one sees that one wind product of Aeolus fits very well to the reference wind profiles while the other one shows considerable deviations (around 10 m/s lower HLOS). This implies regional variations in the wind pattern. As a consequence, the observed outliers in the Aeolus Rayleigh clear winds at 3 and 4.7 km can be attributed to horizontal (and thus also temporal) heterogeneity in the wind field. This behaviour shows the difficulty in comparing Aeolus HLOS winds to the ground-based observations because a perfect co-location in space and time

https://doi.org/10.5194/amt-2022-331
Preprint. Discussion started: 20 December 2022

Atmospheric Measurement Techniques Discussions

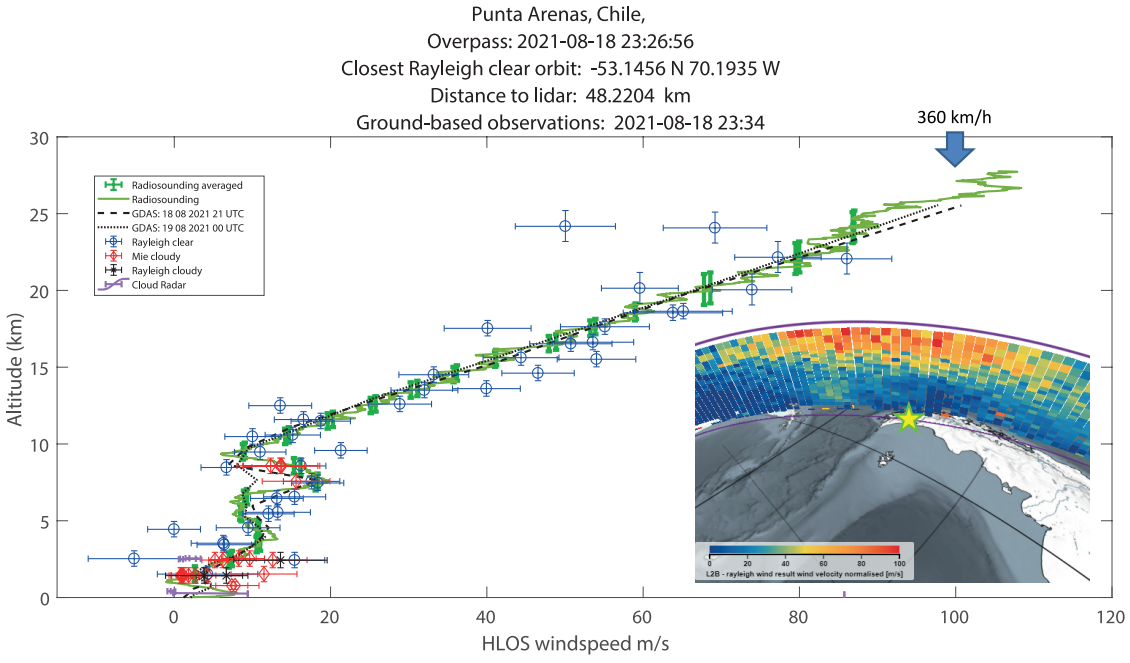

Figure 5. Comparison of Radiosonde, Doppler cloud radar wind and GDAS HLOS winds to Aeolus products on 18 August 2021 - thus representing winter conditions. The Aeolus Rayleigh clear wind curtain for the analysed overpass as visualized with VIRES (Santillan et al., 2019) is shown in the lower right.

can usually never be achieved. However, we are confident that these meteorological variations do not lead to additional biases in the statistics presented in Sec. 5 ff. but are properly covered by the statistical methodologies in terms of random error.

5 Example for statistical validation: Baseline 11 at Leipzig and Punta Arenas

To obtain statistical measures for the performance of Aeolus and its algorithms, we analysed the Aeolus HLOS data by Doppler cloud radar and radiosonde (from now on called reference instruments) as described above for the locations of Leipzig, Germany and Punta Arenas, Chile.

To illustrate that approach, the validation of Aeolus Baseline 11 products around Punta Arenas are shown in Fig. 6. The 1:1 statistic (left column) and the frequency distribution of the deviation from the Doppler cloud radar instrument (reference minus Aeolus, right column) are shown for the Mie (top row) and Rayleigh winds (bottom row). A general good agreement can be seen between Aeolus and the cloud radar being most of the time close to the one-to-one line justifying the use of the orthogonal distance regression (ODR) for fitting the data. The uncertainties of the obtained slopes are thus low (<0.015 m/s for both, Rayleigh clear and Mie cloudy).

More data points could be evaluated for the Mie winds (in total 1817) than for the Rayleigh winds (642), which is a logical

https://doi.org/10.5194/amt-2022-331
Preprint. Discussion started: 20 December 2022

Atmospheric Measurement Techniques Discussions

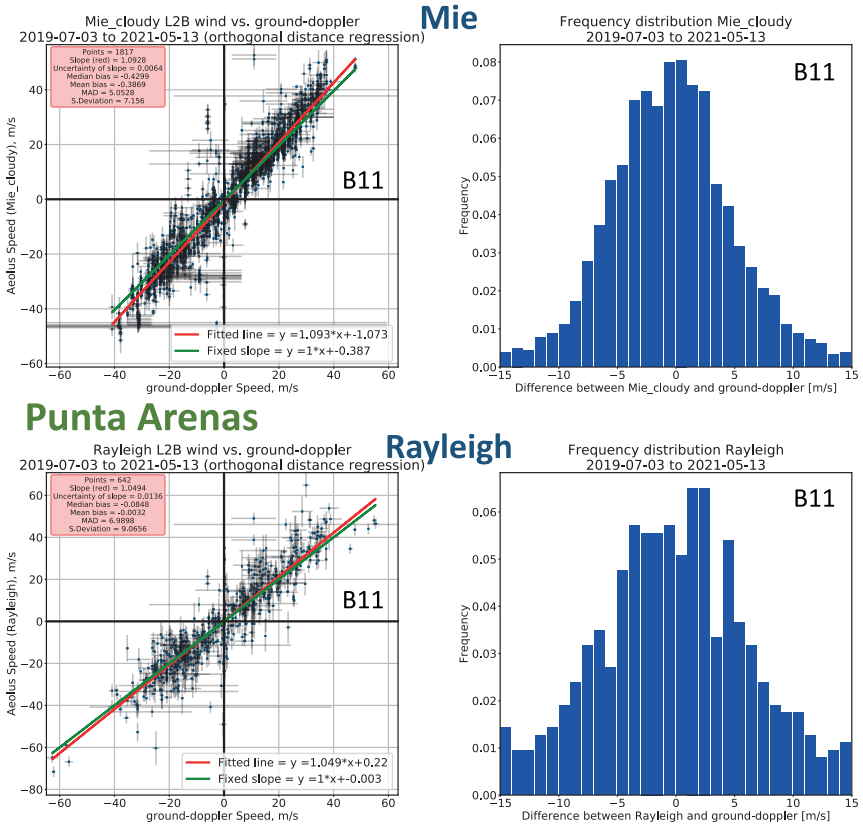

Figure 6. Long-term wind statistic for Baseline 11 for the location of Punta Arenas. Top: Aeolus Mie Wind vs. Ground Doppler Observations, Bottom: Rayleigh Wind vs. Ground Doppler Observations, Left: 1:1 statistic with respective measures, Right: Frequency distribution of differences between the two data sources.

consequence of the higher resolution of the Mie winds and the fact that the cloud radar only derives winds in regions with cloud occurrence. Thus, the validation is more meaningful with respect to Mie winds.

For that wind type, we obtained a slope of 1.1 m/s with the ODR. When forcing the slope to be unity, the resulting offset is equal to the mean bias. A median bias of -0.43 m/s and a mean bias of -0.387 m/s was derived (i.e., Aeolus measures less than the ground-based reference) together with a standard deviation of 7.2 m/s and a scaled median absolute deviation (MAD) of 5.1 m/s. For the Rayleigh wind validation, we obtained respective values of 1.05 m/s (slope), -0.1 m/s (mean bias), -0.003 m/s (median bias), 9.1 m/s (standard deviation) and 7 m/s (scaled MAD) - see statistics box in the left column of Fig. 6.

In the following, we use the scaled MAD as indicator for the random error, in analogy to the median bias for the systematic error also often called bias. The median values are less sensible to outliers than the mean values, but are a valid measure for the uncertainties as long as the frequency distribution is of Gaussian shape. The philosophy of the use of the scaled MAD for Aeolus comparisons is in detail explained in Martin et al. (2021), Lux et al. (2022a), and Weiler et al. (2021a).

https://doi.org/10.5194/amt-2022-331
Preprint. Discussion started: 20 December 2022


Atmospheric Measurement Techniques Discussions

We also performed a Z-score analysis as described in Lux et al. (2022b) and found that, for example, with a Z value of 3 for Baseline 10 , 1.5% of the Aeolus values are identified as outliers. However, in this publication we do not want to discuss the outliers of Aeolus wind products but rather the performance of the publicly available wind data as a whole. Thus, we do not exclude outliers but make a validation of the complete Aeolus data set, given the recommended error thresholds of 8 m/s and 5 m/s for Rayleigh and Mie winds, respectively.

The frequency distribution of the differences (Fig. 6, right) shows a near Gaussian form giving confidence that the statically measures described above could be applied. The obtained systematic error of -0.43 m/s and -0.09 m/s, and the random errors of 5 m/s and 7 m/s for Mie and Rayleigh products, respectively, for Baseline 11 validation at Punta Arenas are in line with other validation activities for this Baseline (Zuo et al., 2022; Geiß et al., 2022). An overview of the main key numbers from this statistic is given in Tab. 2.

We performed the same statistics analysis with the radiosonde data from Leipzig for Baseline 11 - the results are presented in Fig. 7. Giving the fact, that the radiosonde delivers wind data in both, clear and cloudy sky, it becomes clear that this reference instrument is well suited for the Aeolus Rayleigh and Mie wind validation. As radiosondes are not limited to certain atmospheric targets, a coverage up to 25 km could usually be achieved allowing to validate all HLOS winds during an Aeolus overpass. Therefore, results are not confined to the cloud-laden troposphere like in Punta Arenas. Thus, the statistical analysis is more rich in terms of Rayleigh and Mie wind data points as can be seen Fig. 7, left. In total, more than 1500 and 2000 data points could be used for validating the Aeolus Mie and Rayleigh winds, respectively. The frequency distributions of the difference between the reference and Aeolus HLOS winds are of Gaussian shape for, both, Mie and Rayleigh winds and thus gives again evidence for the validity of the applied statistical validation approach. The direct comparison (Fig. 7, left column) shows a general good agreement with only sporadic outliers (e.g., 70 m/s measured by the Aeolus Rayleigh wind product while the radiosonde delivered 15 m/s). The majority of data points are, however, near the imaginary 1:1 line and thus in good agreement. For the Mie winds, we obtained similar values like for Punta Arenas in the Southern Hemisphere, with a systematic error of -0.4 m/s and a random error of 4.6 m/s. For the Rayleigh wind products, we obtained a median bias of -0.5 m/s and a random error similar to the one in Punta Arenas with 5.7 m/s. Giving the fact that more data points are available, the retrieved Rayleigh systematic error for Leipzig is more meaningful even though one has to consider that latitudinal and longitudinal dependencies of the systematic error have been discovered (Martin et al., 2021; Weiler et al., 2021b) and thus single locations like Leipzig and Punta Arenas are not completely representative for the overall global performance of Aeolus. This so-called harmonic oscillating bias was partly resolved due to the M1 temperature correction (Weiler et al., 2021b). However, a leftover effect in this harmonic bias oscillation cannot be ruled out. Especially, if one considers that for Leipzig we could only evaluate the ascending orbit while for Punta Arenas we evaluated both orbit types.

We also performed a radiosonde-based validation for Punta Arenas, but too less data points from the very few radiosonde launches matching the evaluation criteria have been available so that the results are not statistically significant. We thus do not further discuss this specific validation.

A final overview of the obtained metrics for the validation of Baseline 11 is shown in Tab. 2. The same methodology has been applied to the other baselines and will be discussed below.

https://doi.org/10.5194/amt-2022-331
Preprint. Discussion started: 20 December 2022

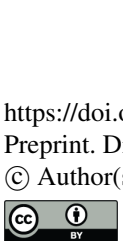

Atmospheric Measurement Techniques Discussions

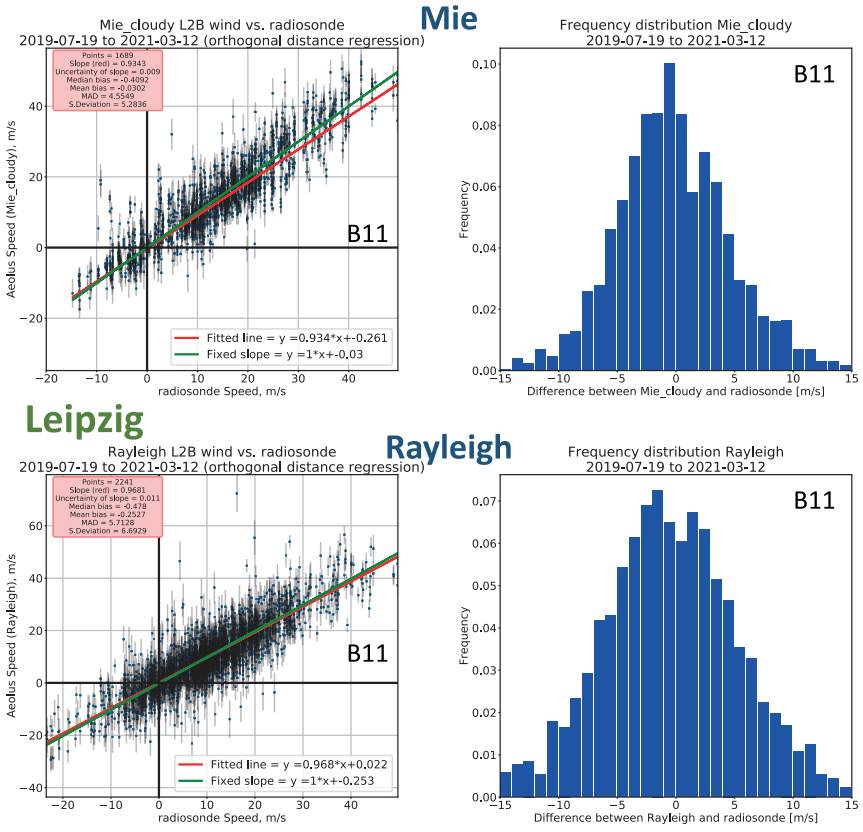

Figure 7. Long-term wind statistic for the Baseline 11 wind validation based on radiosondes at Leipzig. Top: Aeolus Mie Wind vs. Ground Doppler Observations, Bottom: Rayleigh Wind vs. Ground Doppler Observations, Left: 1:1 statistic with respective measures, Right: Frequency distribution of differences between the two data sources.

Table 2. Overview of the metrics obtained for the validation of Baseline 11 at Punta Arenas (left) and Leipzig (right).

(a) Aeolus vs. Cloud radar @ Punta Arenas

	Mie	Rayleigh
Number of points	1817	642
Slope (m/s)	1.09	1.05±0.01
Median bias (m/s)	-0.43	-0.09
Mean bias (m/s)	-0.39	0
Scaled MAD (m/s)	5.05	6.99
Standard deviation (m/s)	7.16	9.07

(b) Aeolus vs. Radiosonde @ Leipzig

	Mie	Rayleigh
Number of points	1689	2241
Slope (m/s)	0.9±0.4	0.97±0.01
Median bias (m/s)	-0.41	-0.48
Mean bias (m/s)	-0.03	-0.25
Scaled MAD (m/s)	4.55	5.71
Standard deviation (m/s)	5.28	6.69

https://doi.org/10.5194/amt-2022-331
Preprint. Discussion started: 20 December 2022

Atmospheric Measurement Techniques Discussions

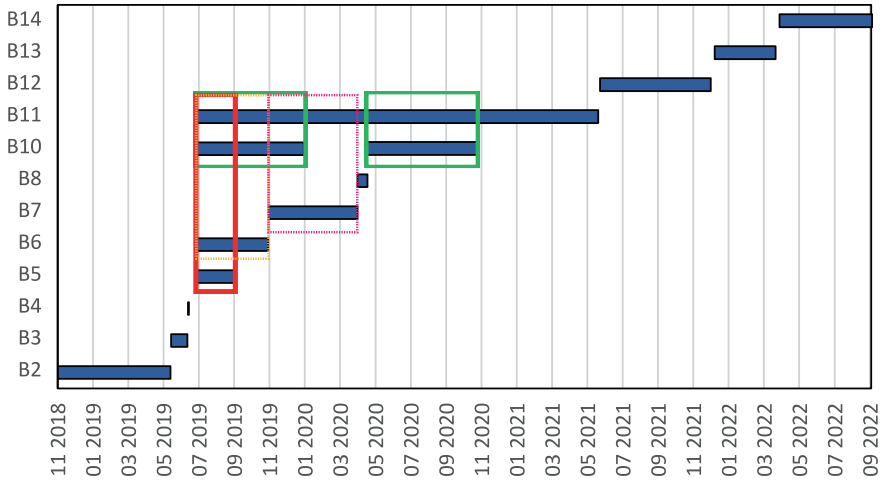

Figure 8. Overview of the different baselines (algorithm versions) which were used to process Aeolus data.

6 Aeolus Validation

We performed the validation analysis for all available baselines, and thus for the time periods listen in Tab. 1 for Punta Arenas (Doppler instruments and radiosonde) and Leipzig (Radiosonde). As stated above in Sec. 3.2, partly reprocessing led to parallel existing products from different algorithm versions for certain time periods. A graphical overview is given in Fig. 8. Depending on the discussion topic further on, we either use different product versions to assess the changes in product quality with changing baseline (Sec. 6.1) or we use the latest algorithm version (baseline) to discuss the performance of the instrument (Sec. 6.2). For example, the periods marked as red, green, and orange rectangles in Fig. 8 are well appropriate and have been used for a baseline inter-comparison. For the "red" period from June 2019 – September 2019, products from four different algorithm versions are available covering already the FM-B era. The orange marked time period covers Baseline 06, 10, and 11 from July 2019 to October 2019 and the magenta-marked period represents the comparison period for B07 to B11 that covers the time from November 2019 to April 2020. The "green" period with 2 different algorithms reaches from June until December 2019 and from May 2020 to October 2020.

6.1 Comparison of Baselines

Due to reprocessing efforts by the Aeolus team, there are certain periods in which Aeolus data is available for different baselines as shown in Fig. 8. This allows to validate the improvements between the different baselines using the same reference data. However, a quantitative measure is not straight forward as due to quality control (QC) procedures etc. not the same amount of Aeolus wind data is available. Nevertheless, it gives a first inside into the improvement made by introducing new baselines.

https://doi.org/10.5194/amt-2022-331
Preprint. Discussion started: 20 December 2022

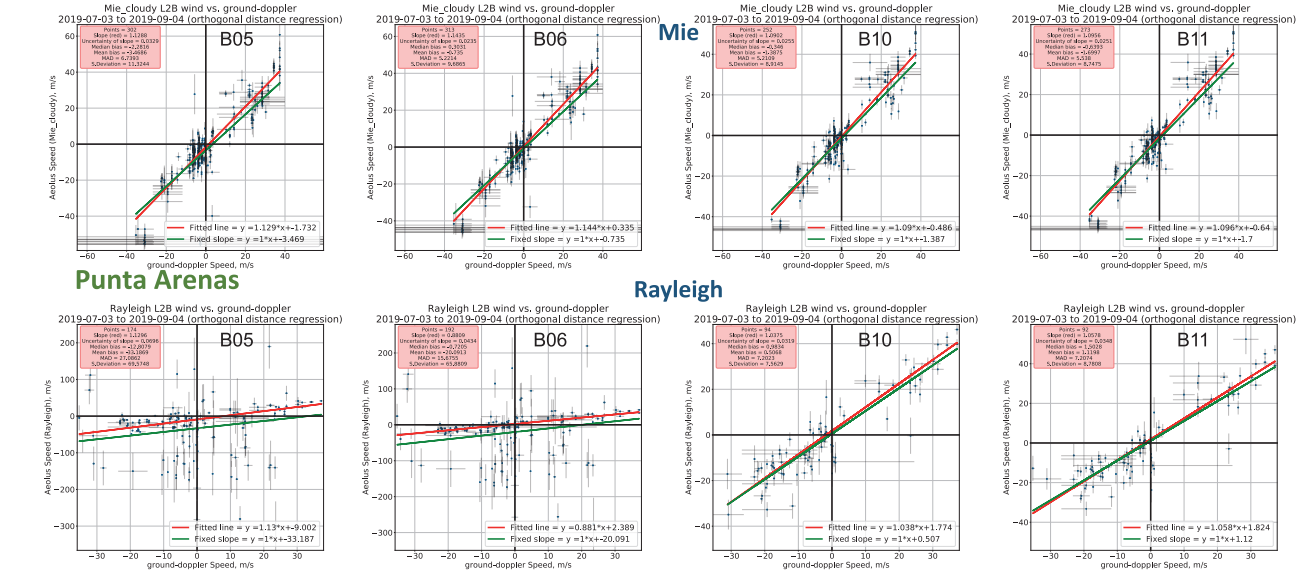

Figure 9. Aeolus performance as obtained by comparison to ground-based Doppler cloud radar in Punta Arenas for Baselines 05, 06, 10, and 11 in the period from July to September 2019.

6.1.1 B05, B06, B10, B11 comparison

To start with the analysis of the different baselines, we focus on the period from July to September 2019 for which data from four different baselines is available: B05, B06, B10, and B11. The switch to laser FM-B was already performed at this time. We analysed this period with the reference data from Punta Arenas and Leipzig. The results for Punta Arenas are shown in Fig. 9 for the Mie (top) and Rayleigh (bottom) wind products.

As this period lasts two months, 16 overpasses in Southern Hemispheric winter could be covered. Without looking at the exact values for the comparison, it gets already obvious that the amount of data which could be compared has significantly lowered from Baseline B05 and B06 to Baseline B10 and B11 - especially evident for the Rayleigh data - indicating improved quality flags and error calculations. Also, the greatest differences can be seen for the Rayleigh winds. At Baseline 05 and 06, many outliers (data not close to the 1:1 line) have been observed, mainly at negative HLOS speeds, which led to a bias of 12 and 10 m/s for B05 and B06, respectively. Random errors are as high as 27 and 15 m/s, respectively. Of course, these numbers have to be assessed with care due to the low number of compared overpasses. Nevertheless, when looking at Baseline 10 and 11, a significant improvement is found. While the number of values to be compared has almost halved, most of the outliers seen in B05 and B06 are removed giving confidence for the improvement of the algorithm including quality control with the new baselines. Especially the introduction of the M1 temperature correction with Baseline 09 seems to have significantly improved the Rayleigh winds. Biases of 1 and 1.3 m/s have been detected with random errors of about 7 m/s for both B10 and B11, respectively. Also here holds that these numbers have to be taken with care due to the relatively low amount of data, but it

https://doi.org/10.5194/amt-2022-331
Preprint. Discussion started: 20 December 2022

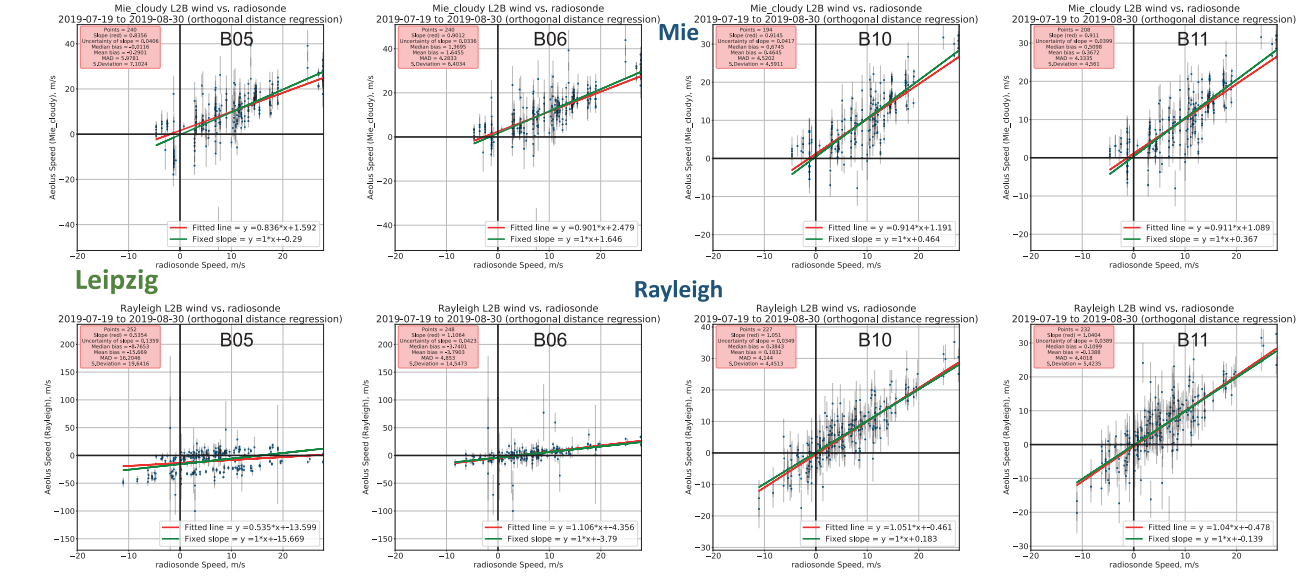

Figure 10. Aeolus performance as obtained by comparison to radiosonde launches in Leipzig for Baselines 05, 06, 10, and 11 in the period from July to September 2019.

definitely shows that algorithms have significantly improved and systematic and random errors are at a good level to allow the use of the Rayleigh wind products.

For the Mie winds, the improvement in performance is also seen, even though it is not as significant as for Rayleigh products, caused by the fact that Mie winds were already much more reliable for B05 and B06 (bias of -2.3 and 0.3 m/s, and random error of 8.7 and 5.2 m/s, respectively). With the introduction of B10 and B11, the median bias is improved to absolute values below 1 m/s with random errors of about 5m/s. For both wind types, the difference between B10 and B11 itself is less significant, most probably caused by the low amount of data which could be used for the comparison. An intense discussion on the B10 to B11 comparison is done later in Sec. 6.1.4 for a longer time period.

For Leipzig, a similar but not equal behaviour was observed as shown in Fig. 10. The number of data points has decreased as well but not as strongly as for Punta Arenas. The magnitude of the systematic and random error for the Mie winds was improved but not as significantly as over Punta Arenas and also the statistical error was lower with increasing baseline for the Mie winds, but one has to state that already Baseline 05 was much more reliable compared to the B05 observations at Punta Arenas.

In contrast, for the Rayleigh winds the bias was high at Baseline 05 (>8m/s) and could be significantly reduced until B11 (<0.2m/s). The major step forward concerning random error for the Rayleigh winds was found since B10, leading to a decrease from 16 m/s to 4 m/s.

https://doi.org/10.5194/amt-2022-331
Preprint. Discussion started: 20 December 2022

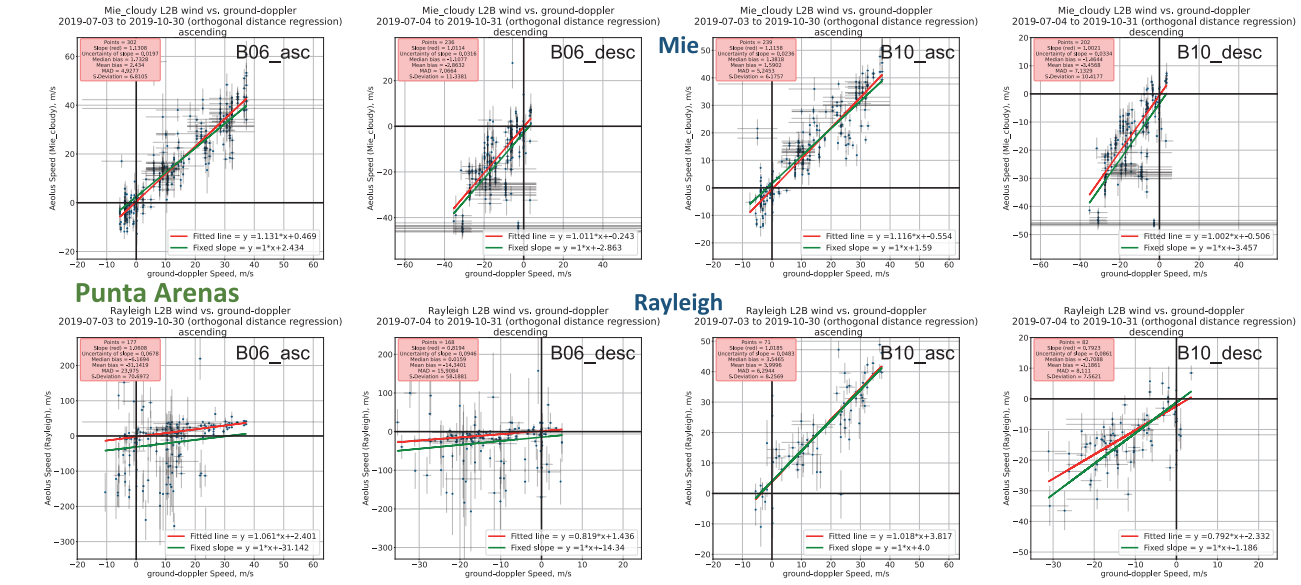

Figure 11. Comparison of Baseline 06 to Baseline 10 in Punta Arenas but separated for ascending and descending orbit type for the period of July to October 2019.

6.1.2 B06 to B10 comparison

The improvement for B10 Rayleigh winds compared to B06 products becomes even more evident if one compares the longer period available for B06 and B10 only, as shown in Fig 11.

Here, the longer time period from July to end of October 2019 could be considered covering 34 overpasses (17 for each orbit type – ascending and descending). Furthermore, the comparison was divided into the orbit types, i.e., if Aeolus measured on an ascending or a descending orbit. Therefore, we also did not include the Leipzig data (on ascending orbit only) in this comparison. At a first glance there are to be no obvious difference in performance of B06 between ascending and descending orbit type for the Rayleigh winds, while the majority of the outliers is seen for Mie winds in the descending orbit. Furthermore, it is also seen that these outliers in the Mie winds remain in Baseline 10, so that one can conclude that there must be other reasons for the discrepancy than the temperature deviation at the Aeolus telescope. For example, it might be atmospheric inhomogeneity which led to the result for which Aeolus measured about -45 m/s but the reference instrument only about -30 m/s.

For the Rayleigh winds, also the amount of data available at B10 decreases by a factor of two compared to B06 but leading to much improved systematic and random errors. At B10, a systematic (random) error of 3.4 (6.2) and -0.7 (8.1) m/s was observed for the ascending and descending Rayleigh winds, respectively, indicating however still a different behaviour between ascending and descending orbits. The same is valid for the Mie winds, with systematic errors of about 1.5 m/s but in different direction.

https://doi.org/10.5194/amt-2022-331
Preprint. Discussion started: 20 December 2022

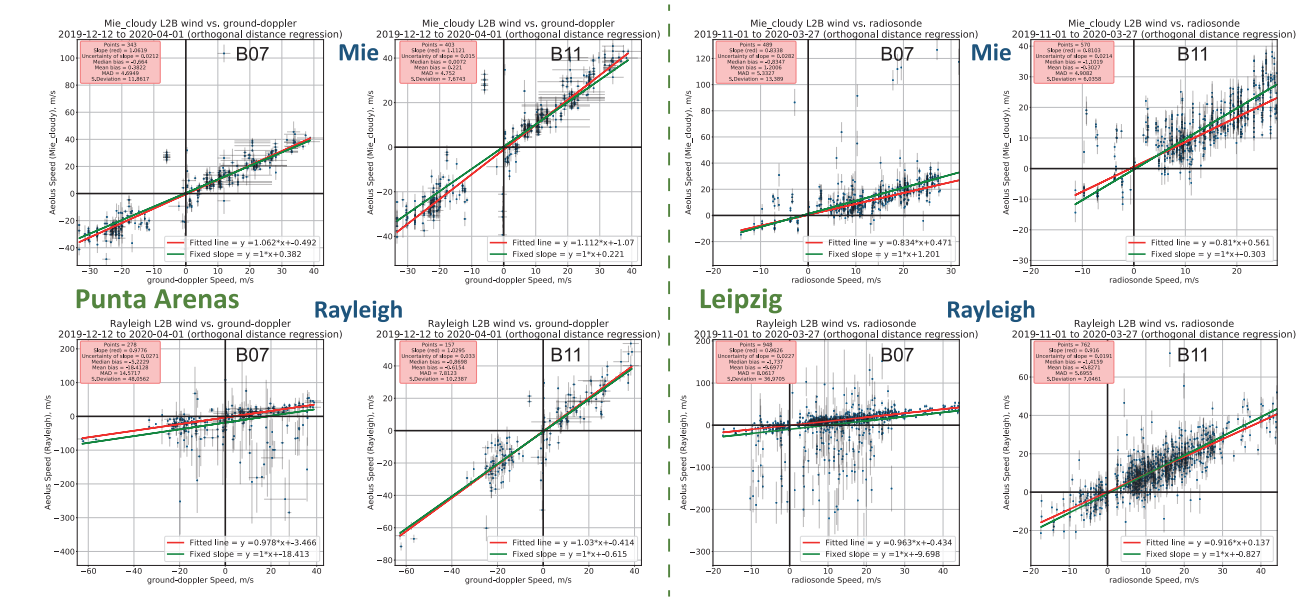

Figure 12. Comparison of the Aeolus performance compared to the reference observations at Punta Arenas (left) and Leipzig (right) for Baselines 07 and 11 in the period from November 2019 to April 2020.

6.1.3 B07 to B11 comparison

We also analysed the difference between B07 and B11 which is given for a longer time series than the comparisons before to analyse the improvement made with the implementation of the M1 telescope temperature correction on a more statistically significant basis. The used data set covers Punta Arenas and Leipzig data from November 2019 to April 2020, thus Southern hemispheric summer and Northern hemispheric winter conditions.

Giving the results presented in Fig. 12, it becomes evident that between B07 and B11, like for B06 to B10, a significant improvement has to be attributed to the Rayleigh wind performance with much less outliers at both locations. Exemplary stated for Punta Arenas only (Fig. 12, left, bottom), a lower systematic (-5.2 vs. -0.9 m/s) and random error (14.6 vs. 7.8 m/s) on the costs of the observations available (157 at B11 compared to 289 at B07) were found. For the Mie wind performance at Punta Arenas (Fig. 12, left, top), the systematic error improved from -0.7 m/s to near 0 while the random error stayed equal with 4.7 m/s with an even increasing number of comparable observations (342 to 403). The number of observations has also increased at Leipzig (Fig. 12, right, top), but with no significant changes in the errors.

As the separation between the ascending and descending orbit is one key element for identifying the harmonic bias effect, we separated the statistics according to that for Punta Arenas observations only and discard the Leipzig data set. The results are shown in Fig. 13.

Without going into too much detail, we could not identify a significant improvement in the performance with respect to the Mie cloudy wind product in this specific data set covering 5 months of observations. Based on more than 150 data points,

https://doi.org/10.5194/amt-2022-331
Preprint. Discussion started: 20 December 2022

Atmospheric Measurement Techniques Discussions

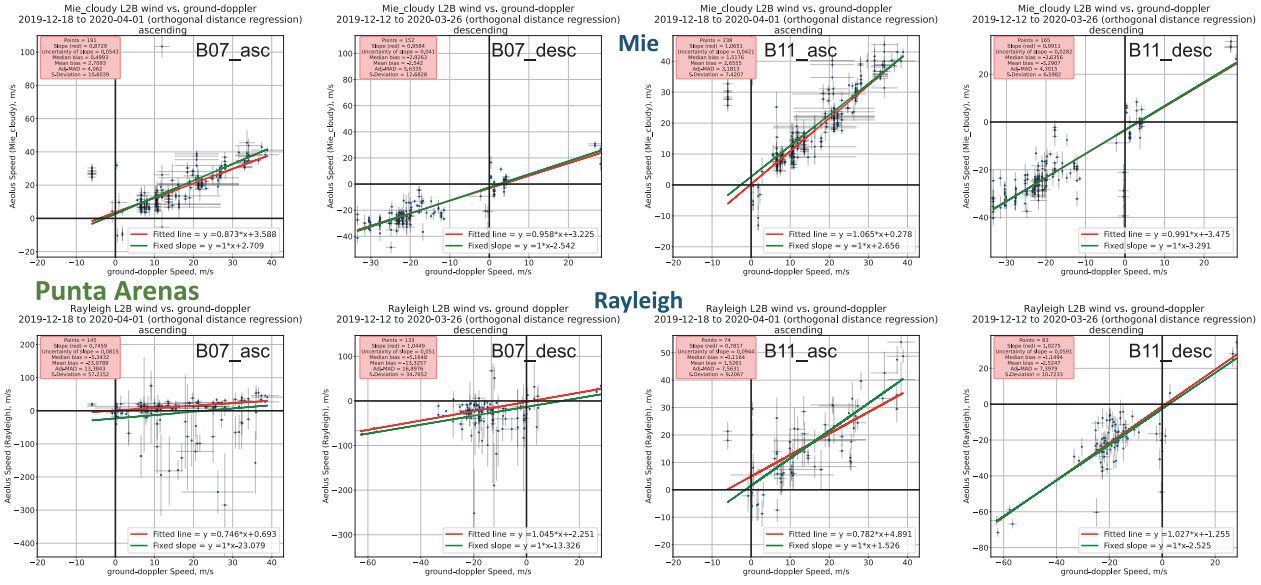

Figure 13. Comparison of Baseline 07 to Baseline 11 in Punta Arenas but separated for ascending and descending orbit type for the period from December 2019 to April 2020.

the Mie systematic error was for B07 +0.5 m/s on the ascending orbit while it was almost -3 m/s on the descending orbit and thus remarkably different. With Baseline 11, however, the differences in the bias have even increased: +1.5 m/s for the ascending orbit and -3.3 m/s for the descending orbit, both for the Mie wind product. Thus, based on this limited data set, no improvement was found for the Mie winds. The Rayleigh winds however, had an equal bias of almost -5 m/s at B07 which significantly decreased to 1.5 m/s and -1.1 m/s (ascending and descending respectively) but on the costs of only half the observations at B11.

These comparisons are not thought as indicator for the Aeolus performance at all, but to show the changes with changing baselines. Having a significant large data set is key to determine statistically significant measures for a single validation site. Therefore, the differences in the overall product performance on a longer time series is made between B10 and B11 in the following.

6.1.4 B10 vs. B11

As stated above, one major improvement step was reached by the introduction of the M1 telescope temperature correction with Baseline 09. Thus, it would be also of interest to compare the algorithm versions beyond this Baseline. This is possible for B10 and B11, for which a significant amount of data is available in parallel as seen in Fig. 8. The most important differences between B10 and B11 is the implementation of the Sat-LOS velocity correction, the reporting Rayleigh spot location and width values, and different Signal-to-Noise Ratio (SNR) thresholds for classification of Mie and Rayleigh (ESA, private communication /confluence).

https://doi.org/10.5194/amt-2022-331
Preprint. Discussion started: 20 December 2022

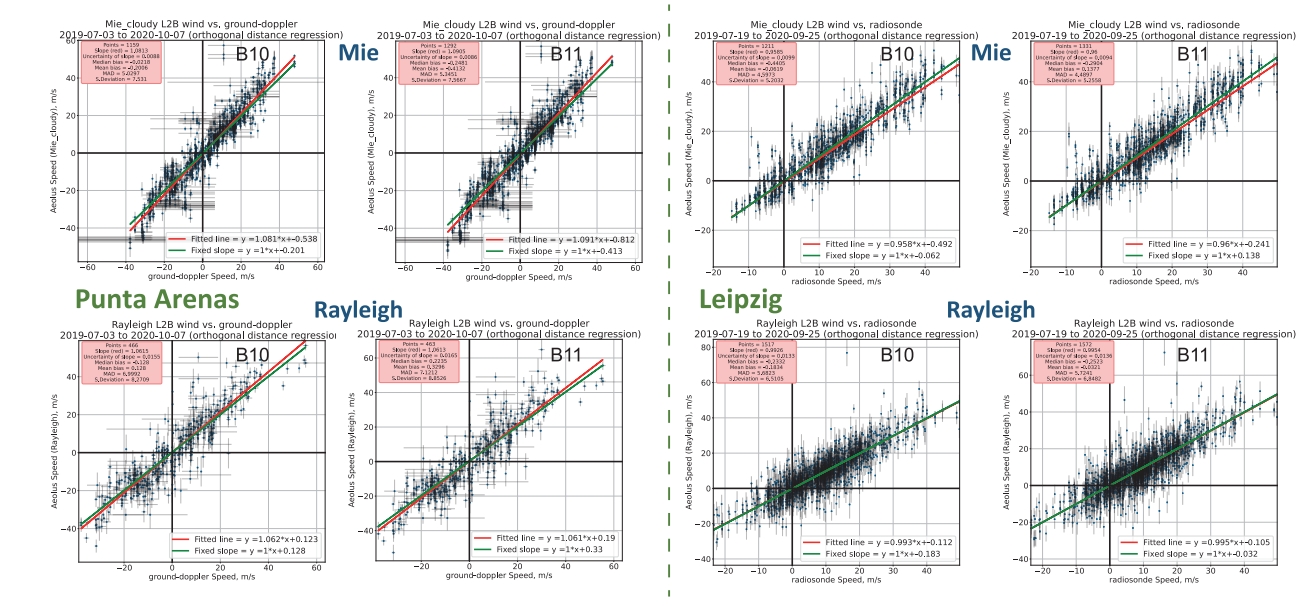

Figure 14. Comparison of the Aeolus performance compared to the reference observations in Punta Arenas (left) and Leipzig (right) for Baselines 10 and 11 in the period from July 2019 to October 2020.

However, giving Fig. 14, left, no significant difference can be found at Punta Arenas between B10 and B11 for both, Mie and Rayleigh wind products, despite the fact that about 10% more Mie winds are available which is most probably due to the new SNR thresholds for the wind type classification. The performance of the Rayleigh winds is indeed slightly worse, but giving the uncertainty not statistically significant. Similar findings are made for Leipzig, Fig. 14, right, for which the radiosondes could cover a much broader height range compared to the cloud radar observations in Punta Arenas but covering only the ascending orbit. Here, the absolute bias has slightly decreased from -0.44 to -0.29 m/s for the Mie winds with similar random error but more measurements at B11 as also observed for Punta Arenas. For Rayleigh winds, no difference at all is seen giving confidence that for this wind type Baseline 10 was already working well over the atmospheric range from 0 to 25 km - at least on Aeolus' ascending orbit over central Europe. If one separates the orbit types for the statistical analysis which is possible for Punta Arenas (Fig. 15), it is interesting to note that still a significant difference in the bias occurs between the two orbit types for both baselines. With respect to the comparison of B10 to B11, for the Mie winds on the ascending orbit, the bias decreased while on the descending orbit it increased (in terms of magnitude) from -1.8 to -2.2 m/s but considering more wind values. For Rayleigh winds, also like in Leipzig, no significant difference is seen at the geographic region of Punta Arenas between the two baselines but also here with significant differences between the orbit types. The random error remained equal between the baselines for both wind types.

https://doi.org/10.5194/amt-2022-331
Preprint. Discussion started: 20 December 2022

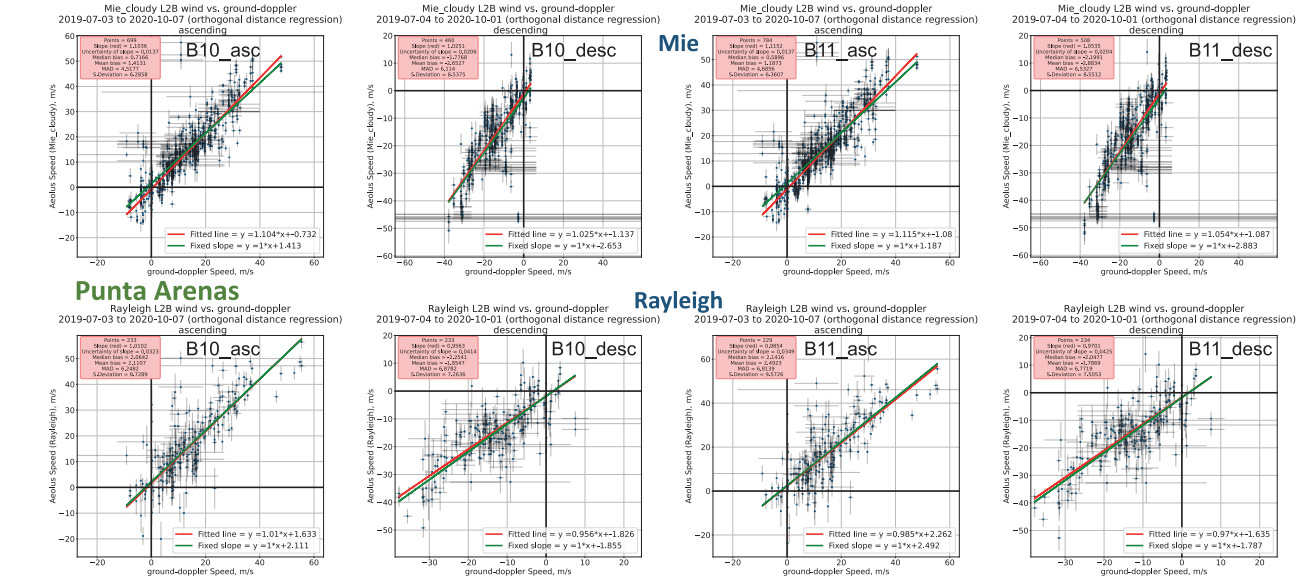

Figure 15. Comparison of Baseline 10 to Baseline 11 in Punta Arenas but separated for ascending and descending orbit type for the period from July 2019 to October 2020.

6.2 Error evolution during lifetime

In the following, we assess the long-term performance of Aeolus. Thus, it is a mix of instrument performance and algorithm improvements.

Figure 16 shows the temporal evolution of the systematic error (median bias, top) and random error (scaled MAD, bottom) for the Mie (left) and Rayleigh (right) products for the full 3-year data set at Punta Arenas. The temporal evolution was computed by using a 28-days moving average window. The most recent available baseline was used and the results are shown for all validation measurements and are split into ascending and descending orbit. At this Southern Hemispheric mid-latitude location, the systematic error of the Mie wind decreased from around 3 m/s towards almost 0 m/s (for the combined observations including both orbit types, yellow color). But a difference between the wind products of the separate two orbit types (purple: descending, pink: ascending) becomes obvious especially for the period between Autumn 2019 and Autumn 2020. Sporadic outliers like September 2020 or April 2021 might be due to certain weather conditions in Punta Arenas. The increase at the end of the observational period in 2021 might be attributed to the orbit shift performed for Aeolus in June 2021 and the resulting larger distances to the validation site. We also had to increase the radius from 100 to 120 km to still be able to validate both orbit types. Thus, the significant increase in magnitude of the systematic error on the descending orbit might be attributed to the increased distance (>100km). The random error of the Mie winds at Punta Arenas varies between 2 and 9 m/s. Here, the decreasing performance of Aeolus with time due to the reduced return signal received at Aeolus (e.g., Parrinello et al., 2022) might be the reason for the increase. Additionally, the random error on the descending orbit has significantly increase since the

https://doi.org/10.5194/amt-2022-331
Preprint. Discussion started: 20 December 2022

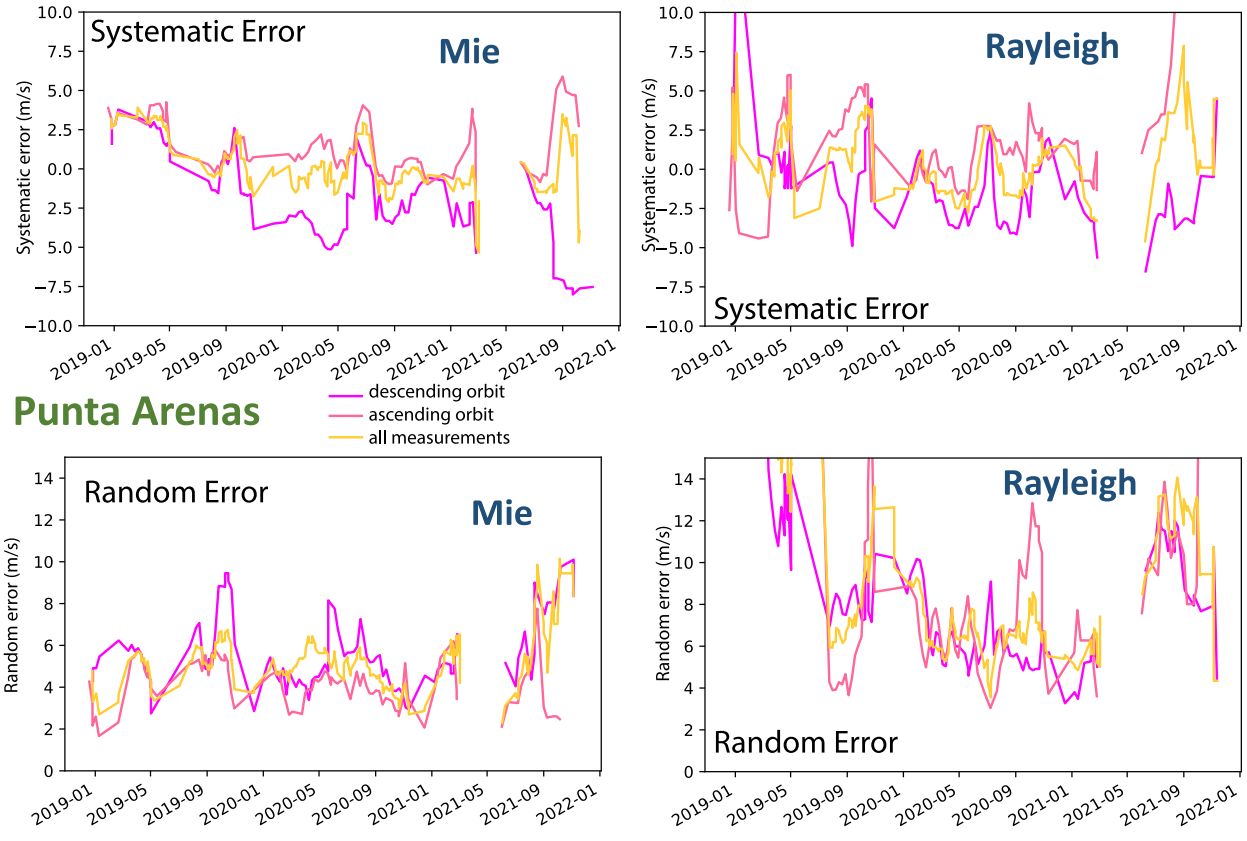

Figure 16. Long term evolution of the derived systematic error (top) and random error (bottom) for the Aeolus Mie (left) and Rayleigh (right) wind products obtained at the Cal/Val station of Punta Arenas for all observations (yellow) and separated by orbit type (ascending: pink, descending: purple). A 28-days moving average window was applied.

orbit shift.

For the Rayleigh winds, a significant improvement in terms of bias can be seen shortly after the start of the observation in beginning of 2019. The systematic error of the Rayleigh wind product seem to fluctuate between -4 and +4 m/s. This indicates that due to the availability of the reference winds in cloudy atmospheric regions only, the statistical significance of the obtained bias at 28-day resolution is reduced. After the orbit shift in June 2019, a significant increased bias was observed but detailed reasons are yet unclear. The random error of the Rayleigh winds has significantly improved in course of the mission lifetime from more than 10 m/s in the beginning of the observations to values of around 5 m/s in the middle of the analysed period. After the orbit shift in June 2021, the random error increased for all orbit types. Note that we here also present Aeolus data which is not yet public, i.e. from the very early mission time and thus this should not be regarded as final performance indicator of Aeolus.

A similar analysis was made for the Leipzig data set, which covers the ascending orbit only but therefore is available until

https://doi.org/10.5194/amt-2022-331
Preprint. Discussion started: 20 December 2022

Atmospheric Measurement Techniques Discussions

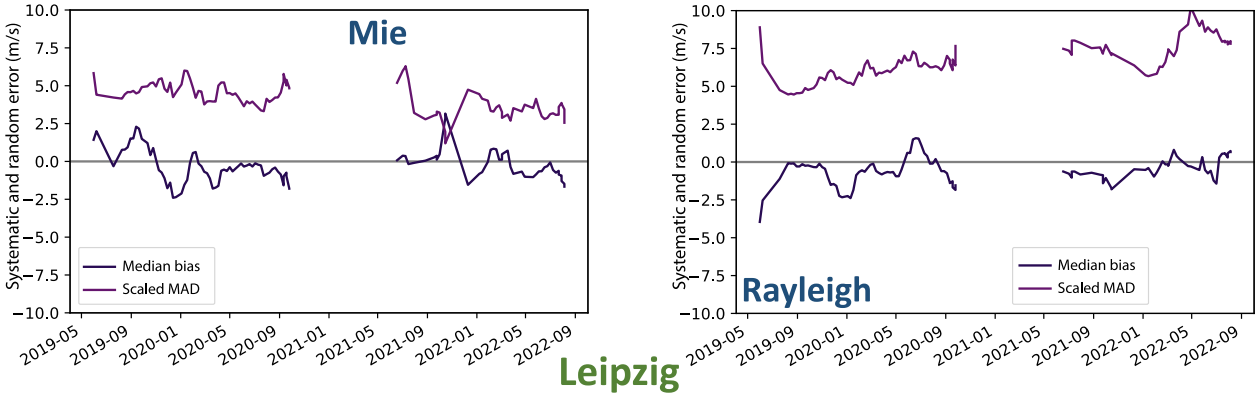

Figure 17. Temporal evolution of the derived systematic error (black - median bias) and random error (purple - scaled MAD) for the Aeolus Mie (left) and Rayleigh (right) wind products obtained at the Cal/Val station of Leipzig (ascending orbit). A 28-days moving average window was applied.

beginning of autumn 2022 (and thus includes Baseline 13 and 14). The results are shown in Fig. 17. Similarly to Punta Arenas, the temporal evolution of the systematic and random error of the Mie and Rayleigh products for Leipzig have been analysed by means of the median bias and the scaled MAD, respectively. A 28-days moving average window was applied. Also at this location, the Mie wind systematic error has significantly decreased with the start of the FM-B period in June 2019. Systematic error values close to 0 m/s were already achieved end of 2019. The random error for the Mie products has been stable at values around 5 m/s until end 2021. Afterwards, it decreased down to 4 m/s. Please note the observational gap which occurred during winter 2020/2021 due to COVID restrictions. Thus, no radiosonde (reference) data was available.

For the Rayleigh winds, also a positive performance trend was observed. The magnitude of the systematic error decreased significantly from values of around 4 m/s to magnitude values below 2 m/s. The random error also decreased until end of 2019 due to performance improvements obtained with the switch to laser FM-B but later continuously increased as a result of the continuously decreasing return signal at Aeolus. The Rayleigh random errors at Leipzig, however, stayed below 10 m/s.

6.3 Validation summary

We performed a validation analysis for both Aeolus wind products (Mie and Rayleigh winds) for the period for which our reference observations (Doppler cloud radar and radiosonde) were available. We thus considered several different baselines (see Tab. 1). The main results in terms of systematic and random error for Punta Arenas (Doppler radar) and Leipzig (Radiosonde) are summarized in Tab. 3 and Tab. 4, respectively. According to Tab. 3, the systematic error of the Aeolus wind products could be significantly lowered with the changes introduced into the processing chain (different baselines). While in the early mission phase, systematic errors of more than 2 m/s (absolute values) were observed for both wind types, these biases could be reduced with the algorithm improvements, such as the M1 temperature correction with Baseline 09. Hence, since Baseline 10, a significant improvement of the Aeolus data was found leading to a low bias (close to 0 m/s) and nearly similar values

https://doi.org/10.5194/amt-2022-331
Preprint. Discussion started: 20 December 2022

Atmospheric Measurement Techniques Discussions

Table 3. Overview of the systematic error (Median Bias) derived with the reference instruments in Punta Arenas and Leipzig for the different baselines. All values are in m/s).

	Punta Arenas		**Leipzig**	
	Rayleigh vs. Doppler	Mie vs. Doppler	Rayleigh vs. Radiosonde	Mie vs. Radiosonde
B02	0.94	2.98	-	-
B06	-3.29	0.76	-3.38	1.39
B07	-5.22	-0.66	-1.74	-0.83
B10	0.18	-0.06	-0.23	-0.44
B11	-0.08	-0.43	-0.48	-0.41
B12	0.55	0.06	-0.86	0.42
B13	-	-	-0.48	-0.03
B14	-	-	-0.3	-0.74

Table 4. Overview of the random error (Scaled MAD) of Aeolus derived from the reference instruments in Punta Arenas and Leipzig for the different baselines. All values are in m/s).

	Punta Arenas		**Leipzig**	
	Rayleigh vs Doppler	Mie vs Doppler	Rayleigh vs Radiosonde	Mie vs Radiosonde
B02	24.9	4.97	-	-
B06	19.53	5.81	5.39	4.71
B07	14.57	4.69	8.06	5.33
B10	6.91	4.91	5.68	4.6
B11	6.99	5.05	5.71	4.55
B12	10.19	4.56	7.34	4.26
B13	-	-	5.89	4.24
B14	-	-	8.67	3.22

https://doi.org/10.5194/amt-2022-331
Preprint. Discussion started: 20 December 2022


Atmospheric Measurement Techniques Discussions

for the mid-latitudinal sites on both hemispheres. As the performance of the laser onboard Aeolus has been getting less ideal (Parrinello et al., 2022), the random errors for the wind products as shown in Tab. 4 are first decreasing with increasing baseline, but later increasing again. However, the systematic error is only slightly affected by this issue, so that one can conclude that the uncertainty introduced by the reduced atmospheric return signal received by Aeolus is mostly affecting the random error - of course on the cost of having less valid wind data, but at least no additional bias seems to be introduced.

7 Conclusions

To validate the novel wind lidar mission Aeolus, we gathered long-term validation data at two mid-latitudinal sites but at different hemispheres. More specifically, we performed regular radiosonde launches for the weekly Aeolus overpasses at Leipzig, Germany (51.35 N, 12.43 E), since May 2019. We also operated a scanning Doppler cloud radar in Punta Arenas, Chile (53.2 S, 70.9 W), so that horizontal wind speed and direction could be retrieved in the vicinity of clouds. Additionally, occasional radiosonde launches were performed. We used all these data sources to validate the overall Aeolus performance with respect to mission time, the algorithm (baseline) version applied to Aeolus data, and the orbit type (ascending, descending, both). It was found that the deviation of the Aeolus HLOS winds from the ground-reference is of Gaussian shape. As systematic error indicator we thus applied the median bias of this distribution while the random error was attributed to the scaled median absolute deviation in accordance to previous validation work on Aeolus and agreement within ESA and DISC (e.g., Lux et al., 2020a). The main findings, i.e. the systematic and random error by baseline, have been summarized in Tab. 3 and Tab. 4. In general, we have found an improving performance of the HLOS wind products with respect to the baseline development. This effect was however partly masked by the effect of lower instrumental performance of Aeolus during its lifetime, especially for the random error. From the whole Aeolus lifetime, we mainly analysed the period which was conducted with the spare laser called FM-B. Even when considering the issues with the lower-than-expected emitted laser energy and the received atmospheric return signal (e.g., Parrinello et al., 2022), which constantly decreased despite many efforts made, we can confirm the general validity of most Aeolus observations during the lifetime. The systematic error of both wind products (Rayleigh clear and Mie cloudy) has significantly decreased as a result of newly introduced baselines with new calibrations and corrections. While at the beginning of the mission, absolute values as high as 5 m/s were observed for the systematic error, it was continuously reduced to values close to 0 m/s before the public release of the Aeolus data in April 2020. This proves the general concept of this space explorer mission to perform active wind observations from space. The random error has been indeed higher than requested by the mission requirements. But compared to the loss in return signal the performing of Aeolus has been still in a range bringing a significant benefit for the numerical weather forecast as demonstrated, e.g., at ECMWF (Rennie et al., 2021), DWD (Martin et al., 2022), and NCMRWF (Rani et al., 2022). The data set gathered at Punta Arenas, Chile and Leipzig, Germany in the course of the validation project EVAA will stay of high value for the Aeolus mission. It can, for example, further be used to validate new algorithm versions applied to historical Aeolus data or to test new methodological approaches. Such efforts will continue even after the satellite has stopped measuring and will help to foster potential follow-on activities for active wind measurements from space as it is currently planned.

https://doi.org/10.5194/amt-2022-331
Preprint. Discussion started: 20 December 2022


Atmospheric Measurement Techniques Discussions

Data availability. The radiosonde data from Leipzig is available at ESA Atmospheric Validation Data Centre (EVDC). Aeolus data is available via ESA Aeolus Online Dissemination System.

Author contributions. HB has conceptualized the study and led the manuscript writing. JW has developed the algorithm for retrieving horizontal wind from ground-based Doppler under the supervision of MR and JB. EB has developed the methodology for the comparison of Aeolus to the ground-reference observations under supervision of HB. JW has finally incorporated these previous works for the long-term analysis under supervision of HB. BB and PS have been responsible for the Punta Arenas operations together with MR and JB, HG for the radiosonde launches in Leipzig. UW contributed her expertise on space-borne profiling and general supervision. All authors have contributed to the intense discussions and the manuscript.

Competing interests. Ulla Wandinger is member of the editorial board of Atmospheric Measurement Techniques. The authors have no further conflict of interest to declare.

Disclaimer. The presented work includes preliminary data (not fully calibrated/validated and not yet publicly released) of the Aeolus mission that is part of the European Space Agency (ESA) Earth Explorer Programme. This includes wind products from processor versions before baseline 10 and/or aerosol and cloud products from before baseline version 11, which have not yet been reprocessed. The processor development, improvement and product reprocessing preparation are performed by the Aeolus DISC (Data, Innovation and Science Cluster), which involves DLR, DoRIT, ECMWF, KNMI, CNRS, S&T, ABB, Serco and TROPOS, in close cooperation with the Aeolus PDGS (Payload Data Ground Segment). The analysis has been performed in the frame of the Aeolus Scientific Calibration and Validation Team (ACVT).

Acknowledgements. Many people are involved in performing the measurements which have been used in this Cal/Val study without whom such an extensive data set would not be possible. It's impossible to list all of them, but I honestly want to acknowledge all the work which is done for installing instruments, keeping measurements running, launching radiosondes and analysing the data. This research has been supported by the German Federal Ministry for Economic Affairs and Energy (BMWi) (grant no. 50EE1721C). Furthermore, we also acknowledge the support through ACTRIS-2 under grant agreement no. 654109 from the European Union's Horizon 2020 research and innovation programme and ACTRIS PPP under the Horizon 2020 – Research and Innovation Framework Programme, H2020-INFRADEV-2016-2017, Grant Agreement number: 7395302. We also appreciate very much the fruitful discussions within the EVAA consortium (LMU, DWD, DLR) and with ESA.

https://doi.org/10.5194/amt-2022-331
Preprint. Discussion started: 20 December 2022

Atmospheric Measurement Techniques Discussions

References

Baars, H., Kanitz, T., Engelmann, R., Althausen, D., Heese, B., Komppula, M., Preißler, J., Tesche, M., Ansmann, A., Wandinger, U., Lim, J.-H., Ahn, J. Y., Stachlewska, I. S., Amiridis, V., Marinou, E., Seifert, P., Hofer, J., Skupin, A., Schneider, F., Bohlmann, S., Foth, A., Bley, S., Pfüller, A., Giannakaki, E., Lihavainen, H., Viisanen, Y., Hooda, R. K., Pereira, S. N., Bortoli, D., Wagner, F., Mattis, I., Janicka, L., Markowicz, K. M., Achtert, P., Artaxo, P., Pauliquevis, T., Souza, R. A. F., Sharma, V. P., van Zyl, P. G., Beukes, J. P., Sun, J., Rohwer, E. G., Deng, R., Mamouri, R.-E., and Zamorano, F.: An overview of the first decade of Polly^{NET}: an emerging network of automated Raman-polarization lidars for continuous aerosol profiling, Atmos. Chem. Phys., 16, 5111–5137, https://doi.org/10.5194/acp-16-5111-2016, 2016.

Baars, H., Geiß, A., Wandinger, U., Herzog, A., Engelmann, R., Bühl, J., Radenz, M., Seifert, P., Althausen, D., Heese, B., Ansmann, A., Martin, A., Leinweber, R., Lehmann, V., Weissmann, M., Cress, A., Filioglou, M., Komppula, M., and Reitebuch, O.: First results from the German Cal/Val activities for Aeolus, EPJ Web Conf., 237, 01 008, https://doi.org/10.1051/epjconf/202023701008, 2020a.

Baars, H., Herzog, A., Heese, B., Ohneiser, K., Hanbuch, K., Hofer, J., Yin, Z., Engelmann, R., and Wandinger, U.: Validation of Aeolus wind products above the Atlantic Ocean, Atmospheric Measurement Techniques, 13, 6007–6024, https://doi.org/10.5194/amt-13-6007-2020, 2020b.

Baars, H., Radenz, M., Floutsi, A. A., Engelmann, R., Althausen, D., Heese, B., Ansmann, A., Flamant, T., Dabas, A., Trapon, D., Reitebuch, O., Bley, S., and Wandinger, U.: Californian wildfire smoke over Europe: A first example of the aerosol observing capabilities of Aeolus compared to ground-based lidar, Geophysical Research Letters, 48, e2020GL092 194, https://doi.org/doi:10.1029/2020GL092194, 2021.

Belova, E., Kirkwood, S., Voelger, P., Chatterjee, S., Satheesan, K., Hagelin, S., Lindskog, M., and Körnich, H.: Validation of Aeolus winds using ground-based radars in Antarctica and in northern Sweden, Atmospheric Measurement Techniques, 14, 5415–5428, https://doi.org/10.5194/amt-14-5415-2021, 2021.

Browning, K. A. and Wexler, R.: The Determination of Kinematic Properties of a Wind Field Using Doppler Radar, Journal of Applied Meteorology and Climatology, 7, 105 – 113, https://doi.org/10.1175/1520-0450(1968)007<0105:TDOKPO>2.0.CO;2, 1968.

Chen, S., Cao, R., Xie, Y., Zhang, Y., Tan, W., Chen, H., Guo, P., and Zhao, P.: Study of the seasonal variation in Aeolus wind product performance over China using ERA5 and radiosonde data, Atmospheric Chemistry and Physics, 21, 11 489–11 504, https://doi.org/10.5194/acp-21-11489-2021, 2021.

de Kloe, J., Stoffelen, A., Tan, D., Andersson, E., Rennie, M., Dabas, A., Poli, P., and Huber, D.: ADM-Aeolus Level-2B/2C Processor Input/Output Data Definitions Interface Control Document, https://earth.esa.int/pi/esa?type=file&table=aotarget&cmd=image&alias=ADM_Aeolus_L2B_Input_Output_DD_ICD, last access: 8 May 2020, 2016.

Dirksen, R. J., Sommer, M., Immler, F. J., Hurst, D. F., Kivi, R., and Vömel, H.: Reference quality upper-air measurements: GRUAN data processing for the Vaisala RS92 radiosonde, Atmos. Meas. Tech., 7, 4463–4490, https://doi.org/10.5194/amt-7-4463-2014, 2014.

ECMWF: Aeolus data impact tests confirm potential of new wind data for NWP, https://www.ecmwf.int/en/about/media-centre/news/2019/aeolus-data-impact-tests-confirm-potential-new-wind-data-nwp, last access: 8 May 2020, 2019a.

ECMWF: Tests show positive impact of new Aeolus wind data on forecasts, https://www.ecmwf.int/en/about/media-centre/news/2019/tests-show-positive-impact-new-aeolus-wind-data-forecasts, last access: 8 May 2020, 2019b.

Engelmann, R., Kanitz, T., Baars, H., Heese, B., Althausen, D., Skupin, A., Wandinger, U., Komppula, M., Stachlewska, I. S., Amiridis, V., Marinou, E., Mattis, I., Linné, H., and Ansmann, A.: The automated multiwavelength Raman polarization and water-vapor lidar Polly^{XT}: the neXT generation, Atmos. Meas. Tech., 9, 1767–1784, https://doi.org/10.5194/amt-9-1767-2016, 2016.

https://doi.org/10.5194/amt-2022-331
Preprint. Discussion started: 20 December 2022

ESA: ADM-Aeolus Science Report, Tech. rep., ESA, https://earth.esa.int/documents/10174/1590943/AEOL002.pdf, last access: 8 May 2020, 2008.

ESA: Aeolus Mission Summary, https://earth.esa.int/web/guest/missions/esa-operational-eo-missions/aeolus/mission-summary, last access: 8 May 2020, 2018.

Fehr, T., Piña, A., Amiridis, V., Baars, H., von Bismarck, J., Borne, M., Cazenave, Q., Chen, S., Flamant, C., Gaetani, M., Knipperz, P., Koopman, R., Lemmerz, C., Marinou, E., Močnik, G., Parrinello, T., Reitebuch, O., Skofronick-Jackson, G., Straume, A. G., and Zenk, C.: The Joint Aeolus Tropical Atlantic Campaign – First results for Aeolus calibration/validation and science in the tropics, ESA Atmospheric Science Conference (2021), Online, 22.–26. November 2021, 2021.

Flament, T., Dabas, A., Trapon, D., Lacour, A., Ehlers, F., Baars, H., and Huber, D.: Aeolus aerosol and cloud product, in: EGU General Assembly 2021 (Online), European Geosciences Union, https://doi.org/doi:10.5194/egusphere-egu21-14390, 2021.

Geiß, A., Martin, A., Lehmann, V., Leinweber, R., Reitebuch, O., and Weissmann, M.: Long-term validation of the Aeolus L2B wind product with the German radar wind profiler network, in: Aeolus 3rd Anniversary Conference, Taormina, Italy, 2022.

Görsdorf, U., Lehmann, V., Bauer-Pfundstein, M., Peters, G., Vavriv, D., Vinogradov, V., and Volkov, V.: A 35-GHz Polarimetric Doppler Radar for Long-Term Observations of Cloud Parameters—Description of System and Data Processing, Journal of Atmospheric and Oceanic Technology, 32, 675 – 690, https://doi.org/10.1175/JTECH-D-14-00066.1, 2015.

Hagelin, S., Azad, R., Lindskog, M., Schyberg, H., and Körnich, H.: Evaluating the use of Aeolus satellite observations in the regional numerical weather prediction (NWP) model Harmonie–Arome, Atmospheric Measurement Techniques, 14, 5925–5938, https://doi.org/10.5194/amt-14-5925-2021, 2021.

Illingworth, A., Hogan, R., O'connor, E., Bouniol, D., Brooks, M., Delanoë, J., Donovan, D., Eastment, J., Gaussiat, N., Goddard, J., et al.: Cloudnet: Continuous evaluation of cloud profiles in seven operational models using ground-based observations, Bulletin of the American Meteorological Society, 88, 883–898, 2007.

Iwai, H., Aoki, M., Oshiro, M., and Ishii, S.: Validation of Aeolus Level 2B wind products using wind profilers, ground-based Doppler wind lidars, and radiosondes in Japan, Atmospheric Measurement Techniques, 14, 7255–7275, https://doi.org/10.5194/amt-14-7255-2021, 2021.

Jauhiainen, H., Survo, P., Lehtinen, R., and Lentonen, J.: Radiosonde RS41 and RS92 key differences and comparison test results in different locations and climates, in: TECO-2014, WMO Technical Conference on Meteorological and Environmental Instruments and Methods of Observations, Saint Petersberg, Russia, https://www.wmo.int/pages/prog/www/IMOP/publications/IOM-116_TECO-2014/Session%203/P3_16_Juhiainen_Radiosonde_RS41_RS92_Key_Differences_Comparison_TestResults.pdf, last access: 8 May 2020, 2014.

Jensen, M. P., Holdridge, D. J., Survo, P., Lehtinen, R., Baxter, S., Toto, T., and Johnson, K. L.: Comparison of Vaisala radiosondes RS41 and RS92 at the ARM Southern Great Plains site, Atmos. Meas. Tech., 9, 3115–3129, https://doi.org/10.5194/amt-9-3115-2016, 2016.

Krisch, I., Lemmerz, C., Lux, O., Marksteiner, U., Reitebuch, O. Weiler, F., Witschas, B., Bracci, F., Meringer, M., Schmidt, K. Huber, D., Nikolaus, I., Vaughan, M., Dabas, A., Flament, T., Trapon, D., Isaksen, L., Rennie, M. Abdalla, S., Donovan, D., de Kloe, J., Marseille, G.-J., Stoffelen, A., Wernham, D., Kanitz, T., Straume, A.-G., von Bismarck, J., Bley, S., Fischer, P., and Parrinello, T.: Data quality of Aeolus wind measurements, in: EGU General Assembly 2020, Online, 4-8 May 2020, https://doi.org/10.5194/egusphere-egu2020-18186, 2020.

Liu, H., Garrett, K., Ide, K., Hoffman, R. N., and Lukens, K. E.: A statistically optimal analysis of systematic differences between Aeolus horizontal line-of-sight winds and NOAA's Global Forecast System, Atmospheric Measurement Techniques, 15, 3925–3940, https://doi.org/10.5194/amt-15-3925-2022, 2022.

https://doi.org/10.5194/amt-2022-331
Preprint. Discussion started: 20 December 2022

Lux, O., Lemmerz, C., Weiler, F., Marksteiner, U., Witschas, B., Rahm, S., Geiß, A., and Reitebuch, O.: Intercomparison of wind observations from the European Space Agency's Aeolus satellite mission and the ALADIN Airborne Demonstrator, Atmos. Meas. Tech., 13, 2075–2097, https://doi.org/10.5194/amt-13-2075-2020, 2020a.

Lux, O., Wernham, D., Bravetti, P., McGoldrick, P., Lecrenier, O., Riede, W., D'Ottavi, A., Sanctis, V. D., Schillinger, M., Lochard, J., Marshall, J., Lemmerz, C., Weiler, F., Mondin, L., Ciapponi, A., Kanitz, T., Elfving, A., Parrinello, T., and Reitebuch, O.: High-power and frequency-stable ultraviolet laser performance in space for the wind lidar on Aeolus, Opt. Lett., 45, 1443–1446, https://doi.org/10.1364/OL.387728, 2020b.

Lux, O., Lemmerz, C., Weiler, F., Marksteiner, U., Witschas, B., Rahm, S., Geiß, A., Schäfler, A., and Reitebuch, O.: Retrieval improvements for the ALADIN Airborne Demonstrator in support of the Aeolus wind product validation, Atmospheric Measurement Techniques, 15, 1303–1331, https://doi.org/10.5194/amt-15-1303-2022, 2022a.

Lux, O., Witschas, B., Geiß, A., Lemmerz, C., Weiler, F., Marksteiner, U., Rahm, S., Schäfler, A., and Reitebuch, O.: Quality control and error assessment of the Aeolus L2B wind results from the Joint Aeolus Tropical Atlantic Campaign, Atmospheric Measurement Techniques, 15, 6467–6488, https://doi.org/10.5194/amt-15-6467-2022, 2022b.

Martin, A., Weissmann, M., Reitebuch, O., Rennie, M., Geiß, A., and Cress, A.: Validation of Aeolus winds using radiosonde observations and numerical weather prediction model equivalents, Atmospheric Measurement Techniques, 14, 2167–2183, https://doi.org/10.5194/amt-14-2167-2021, 2021.

Martin, A., Weissmann, M., and Cress, A.: Investigation of dynamical scenarios leading to particularly high impact of Aeolus on NWP forecasts, EGUsphere, 2022, 1–23, https://doi.org/10.5194/egusphere-2022-1150, 2022.

Parrinello, T., Straume, A. G., Von Bismark, J., Tran, V., Romanazzo, M., Wernham, D., Krisna, T. C., Sathe, A., Colangeli, G., Garsva, S., Fehr, T., Krisch, I. Reitebuch, O., and Rennie, M.: Aeolus: ESA's wind mission3+ years in space. Status and future challenges, in: ESA Living Planet Symposium 2022, Bonn, Germany, https://earth.esa.int/living-planet-symposium-2022-presentations/25.05.Wednesday/Nairobi_1-2/0830-1010/01_Parrinello_Session_B2_11_Version_3.pdf, last access: 25 November 2022, 2022.

Päschke, E., Leinweber, R., and Lehmann, V.: An assessment of the performance of a 1.5 μ m Doppler lidar for operational vertical wind profiling based on a 1-year trial, Atmospheric Measurement Techniques, 8, 2251–2266, https://doi.org/10.5194/amt-8-2251-2015, 2015.

Radenz, M., Bühl, J., Seifert, P., Baars, H., Engelmann, R., Barja González, B., Mamouri, R.-E., Zamorano, F., and Ansmann, A.: Hemispheric contrasts in ice formation in stratiform mixed-phase clouds: disentangling the role of aerosol and dynamics with ground-based remote sensing, Atmospheric Chemistry and Physics, 21, 17 969–17 994, https://doi.org/10.5194/acp-21-17969-2021, 2021.

Rani, S. I., Jangid, B. P., Kumar, S., Bushair, M. T., Sharma, P., George, J. P., George, G., and Das Gupta, M.: Assessing the quality of novel Aeolus winds for NWP applications at NCMRWF, Quarterly Journal of the Royal Meteorological Society, 148, 1344–1367, https://doi.org/https://doi.org/10.1002/qj.4264, 2022.

Ratynski, M., Khaykin, S., Hauchecorne, A., Wing, R., Cammas, J.-P., Hello, Y., and Keckhut, P.: Validation of Aeolus wind profiles using ground-based lidar and radiosonde observations at La Réunion Island and the Observatoire de Haute Provence, EGUsphere, 2022, 1–33, https://doi.org/10.5194/egusphere-2022-822, 2022.

Ray, P. S. and Ziegler, C.: De-Aliasing First-Moment Doppler Estimates, Journal of Applied Meteorology and Climatology, 16, 563 – 564, https://doi.org/10.1175/1520-0450(1977)016<0563:DAFMDE>2.0.CO;2, 1977.

Reitebuch, O.: The Spaceborne Wind Lidar Mission ADM-Aeolus, in: Atmospheric Physics: Background – Methods – Trends, edited by Schumann, U., pp. 815–827, Springer, https://doi.org/10.1007/978-3-642-30183-4_49, 2012.

https://doi.org/10.5194/amt-2022-331
Preprint. Discussion started: 20 December 2022

Reitebuch, O., Lemmerz, C., Lux, O., Marksteiner, U., Rahm, S., Weiler, F., Witschas, B., Meringer, M., Schmidt, K., Huber, D., Nikolaus, I., Geiß, A., Vaughan, M., Dabas, A., Flament, T., Stieglitz, H., Isaksen, L., Rennie, M., de Kloe, J., Marseille, G.-J., Stoffelen, A., Wernham, D., Kanitz, T., Straume, A.-G., Fehr, T., von Bismark, J., Floberghagen, R., and Parrinello, T.: Initial assessment of the performance of the first Wind Lidar in space on Aeolus, EPJ Web Conf., 237, 01 010, https://doi.org/10.1051/epjconf/202023701010, 2020.

Rennie, M. and Isaksen, L.: The NWP impact of Aeolus Level-2B Winds at ECMWF, https://doi.org/10.21957/alift7mhr, 2020.

Rennie, M. P., Isaksen, L., Weiler, F., de Kloe, J., Kanitz, T., and Reitebuch, O.: The impact of Aeolus wind retrievals on ECMWF global weather forecasts, Quarterly Journal of the Royal Meteorological Society, 147, 3555–3586, https://doi.org/https://doi.org/10.1002/qj.4142, 2021.

Santillan, D., Huber, D., Meringer, M., Reitebuch, O., Schindler, F., and Weiler, F.: VirES for Aeolus - Online visual analysis of Aeolus data, in: ESA Living Planet Symposium 2019, Milan, Italy, https://elib.dlr.de/130561/, last access: 8 May 2020, 2019.

Seifert, P., Radenz, M., Barja Gonzalez, B., Kalesse, H., Stratmann, F., Bühl, J., Teisseire, A., Vogl, T., Jimenez, C., Ohneiser, K., Schimmel, W., Wex, H., Ataei, F., Gong, X., Floutsi, A., Engelmann, R., Baars, H., Witthuhn, J., Ansmann, A., and Zamorano, F.: Aerosol, clouds, dynamics and their interaction over Punta Arenas, Chile (53°S, 71°W): A summary of two years of remote sensing and in-situ observations in the frame of DACAPO-PESO, in: 2020 AGU Fall Meeting, 2020.

Simonelli, G., Brandt, C., and Rezazad, M.: Aeolus First Year in Orbit Power System Performance, in: 2019 European Space Power Conference (ESPC), Juan-les-Pins, France, pp. 1–4, https://doi.org/10.1109/ESPC.2019.8932017, 2019.

Siomos, N., Gkikas, A., Baars, H., Wandinger, U., Amiridis, V., Paschou, P., and EARLINET-Consortium: Investigating the performance of AEOLUS L2A products over Europe with EARLINET ground-based lidars, in: EGU General Assembly 2021 (Online), European Geosciences Union, https://doi.org/doi:10.5194/egusphere-egu21-12460, 2021.

Stoffelen, A., Pailleux, J., Källén, E., Vaughan, J. M., Isaksen, L., Flamant, P., Wergen, W., Andersson, E., Schyberg, H., Culoma, A., Meynart, R., Endemann, M., and Ingmann, P.: The Atmospheric Dynamics Mission for Global Wind Field Measurment, Bull. Amer. Meteor. Soc., 86, 73–88, https://doi.org/10.1175/BAMS-86-1-73, 2005.

Stoffelen, A., Marseille, G. J., Bouttier, F., Vasiljevic, D., de Haan, S., and Cardinali, C.: ADM-Aeolus Doppler wind lidar Observing System Simulation Experiment, Q. J. R. Meteorol. Soc., 132, 1927–1947, https://doi.org/10.1256/qj.05.83, 2006.

Straume, A. G., Rennie, M., Isaksen, L., de Kloe, J., Marseille, G.-J., Stoffelen, A., Flament, T., Stieglitz, H., Dabas, A., Huber, D., Reitebuch, O., Lemmerz, C., Lux, O., Marksteiner, U., Weiler, F., Witschas, B., Meringer, M., Schmidt, K., Nikolaus, I., Geiß, A., Flamant, P., Kanitz, T., Wernham, D., von Bismarck, J., Bley, S., Fehr, T., Floberghagen, R., and Parrinello, T.: ESA's space-based Doppler wind lidar mission Aeolus – First wind and aerosol product assessment results, EPJ Web Conf., 237, 01 007, https://doi.org/10.1051/epjconf/202023701007, 2020.

Tabary, P., Scialom, G., and Germann, U.: Real-Time Retrieval of the Wind from Aliased Velocities Measured by Doppler Radars, Journal of Atmospheric and Oceanic Technology, 18, 875 – 882, https://doi.org/10.1175/1520-0426(2001)018<0875:RTROTW>2.0.CO;2, 2001.

Tan, D. G. H., Andersson, E., De Kloe, J., Marseille, G.-J., Stoffelen, A., Poli, P., Denneulin, M.-L., Dabas, A., Huber, D., Reitebuch, O., Flamant, P., Le Rille, O., and Nett, H.: The ADM-Aeolus wind retrieval algorithms, Tellus A, 60, 191–205, https://doi.org/10.1111/j.1600-0870.2007.00285.x, 2008.

Tukiainen, S., O'connor, E., and Korpinen, A.: CloudnetPy: A Python package for processing cloud remote sensing data, Journal of Open Source Software, 5, 2123, 2020.

https://doi.org/10.5194/amt-2022-331
Preprint. Discussion started: 20 December 2022

Weiler, F., Kanitz, T., Wernham, D., Rennie, M., Huber, D., Schillinger, M., Saint-Pe, O., Bell, R., Parrinello, T., and Reitebuch, O.: Characterization of dark current signal measurements of the ACCDs used on board the Aeolus satellite, Atmospheric Measurement Techniques, 14, 5153–5177, https://doi.org/10.5194/amt-14-5153-2021, 2021a.

Weiler, F., Rennie, M., Kanitz, T., Isaksen, L., Checa, E., de Kloe, J., Okunde, N., and Reitebuch, O.: Correction of wind bias for the lidar on board Aeolus using telescope temperatures, Atmospheric Measurement Techniques, 14, 7167–7185, https://doi.org/10.5194/amt-14-7167-2021, 2021b.

Witschas, B., Lemmerz, C., Geiß, A., Lux, O., Marksteiner, U., Rahm, S., Reitebuch, O., and Weiler, F.: First validation of Aeolus wind observations by airborne Doppler wind lidar measurements, Atmospheric Measurement Techniques, 13, 2381–2396, https://doi.org/10.5194/amt-13-2381-2020, 2020.

Witschas, B., Lemmerz, C., Geiß, A., Lux, O., Marksteiner, U., Rahm, S., Reitebuch, O., Schäfler, A., and Weiler, F.: Validation of the Aeolus L2B wind product with airborne wind lidar measurements in the polar North Atlantic region and in the tropics, Atmospheric Measurement Techniques Discussions, 2022, 1–32, https://doi.org/10.5194/amt-2022-233, 2022.

Wu, S., Sun, K., Dai, G., Wang, X., Liu, X., Liu, B., Song, X., Reitebuch, O., Li, R., Yin, J., and Wang, X.: Inter-comparison of wind measurements in the atmospheric boundary layer and the lower troposphere with Aeolus and a ground-based coherent Doppler lidar network over China, Atmospheric Measurement Techniques, 15, 131–148, https://doi.org/10.5194/amt-15-131-2022, 2022.

Zuo, H., Hasager, C. B., Karagali, I., Stoffelen, A., Marseille, G.-J., and de Kloe, J.: Evaluation of Aeolus L2B wind product with wind profiling radar measurements and numerical weather prediction model equivalents over Australia, Atmospheric Measurement Techniques, 15, 4107–4124, https://doi.org/10.5194/amt-15-4107-2022, 2022.